

AD612178

Annual Report

January 1, 1964 - December 31, 1964

RESEARCH ON UNSTABLE COMBUSTION
IN SOLID PROPELLANT ROCKETS

Prepared for:

AIR FORCE OFFICE OF SCIENTIFIC RESEARCH
WASHINGTON, D.C. 20333

Sponsored by:

ADVANCED RESEARCH PROJECTS AGENCY
ARPA ORDER NO. 317, AMEND. NO. 11

CONTRACT NO. AF 49(638)-1367

STANFORD RESEARCH INSTITUTE

(MENLO PARK, CALIFORNIA

*SRI

STANFORD RESEARCH INSTITUTE

MENLO PARK, CALIFORNIA



January 13, 1965

Annual Report

January 1, 1964 – December 31, 1964

RESEARCH ON UNSTABLE COMBUSTION
IN SOLID PROPELLANT ROCKETS

Prepared for:

AIR FORCE OFFICE OF SCIENTIFIC RESEARCH
WASHINGTON, D.C. 20333

Sponsored by:

ADVANCED RESEARCH PROJECTS AGENCY
ARPA ORDER NO. 317, AMEND. NO. 11

CONTRACT NO. AF 49(638)-136.

By: L. A. DICKINSON E. L. CAPENER R. J. KIER

SRI Project PRU-4865

Approved: LIONEL A. DICKINSON, ASSOCIATE DIRECTOR
PROPULSION SCIENCES

Copy No. 122.

ABSTRACT

Initiation of axial combustion instability in an experimental combustor, 40 inches long by 50 inches I.D., containing a radial burning grain, has been studied utilizing a wide variety of composite propellants. Where instability occurred, a correlation was found between the threshold pressure at which instability was first observed and propellant ballistic parameters, notably the linear burning rate. Fast burning propellants, containing either a catalyst or potassium perchlorate, did not sustain axial mode combustion instability. Transverse instability was observed for most non-aluminized propellants in pressure regimes where they were stable to axial combustion instability.

An explanation of combustion stability criteria has been sought in terms of either mixing processes within a granular diffusion flame or a thermal explosion process. The granular diffusion flame concept appears thus far to be the more promising explanation; it predicts the stability trends observed in large solid propellant rocket motors.

CONTENTS

ABSTRACT	ii
LIST OF ILLUSTRATIONS.	v
LIST OF TABLES	vii
I INTRODUCTION.	1
II RESEARCH OBJECTIVES	4
III EXPERIMENTAL PROGRAM.	5
Experimental Method	5
Propellants Investigated.	10
IV EXPERIMENTAL RESULTS.	14
Data on Compositional Factors Study	14
Ammonium Perchlorate-Based Propellants.	14
Principal Observations Relating to Ammonium Perchlorate-Based Propellants	18
Mixed Oxidizer Propellants.	18
Propellants Based on Different Oxidizers.	20
High Energy Double-Base Propellants	21
Transverse Instability and Associated Phenomena.	21
Motor Dimensional Parameters and Combustion Instability .	25
Grain Geometry Factors.	26
Window Motor Studies.	27
Wave Phenomena.	28
V DISCUSSION AND APPLICATION OF SIGNIFICANT RESEARCH FINDINGS .	29
Characteristic Combustion Time Relationship	29
Stability Bound Analysis.	38
Discussion of Compositional Factors	42
Acoustical Instability Theory	42

CONTENTS (Concl'd)

Application of Experimental Results to Design and Scaling of Rocket Motors.	43
VI CONCLUDING REMARKS	46
ACKNOWLEDGMENTS	46
REFERENCES	47
APPENDIX A.	A-1
APPENDIX B.	B-1

LIST OF ILLUSTRATIONS

Fig. 1	Selection of Threshold Point, by Extrapolating Unstable Data Points Back to Stable " K_n vs. P" Plot (Threshold burning rate obtained from associated burning rate data).	6
Fig. 2	Instrumentation Block Diagram.	7
Fig. 3	5-inch x 40-inch Unstable Combustion Motor Assembly.	9
Fig. 4	Experimental 2-inch x 20-inch Window Motor	10
Fig. 5a	Initiation of Instability on Initial Pulse (5 inch by 40 inch motor composition PBAN 162)	15
Fig. 5b	Initiation of Instability on Terminal Pulse (5 inch by 40 inch motor composition PBAN 162)	15
Fig. 6	Correlation of Threshold Pressure with Propellant Burning Rate 5-inch x 40-inch Rocket Motor	17
Fig. 7	Threshold Data for Mixed Oxidizer Propellants.	19
Fig. 8	Firing Record for Ammonium Nitrate Propellant Grain (First 2 Seconds Show Burning of Starter Grain). Pulses as Coded 1, 2, 3, & 4.	20
Fig. 9	Typical Propellant Burning Rates; Solid Line Stable Regime, Dotted Line Unstable Regime for 5-inch x 40-inch Motor.	22
Fig. 10	Aluminized Nitrasol Propellant, NIT 101, Exhibiting First Axial Mode (500 cps) and Then a High Frequency Instability (>10 Kc).	23
Fig. 11	Opposed Slab Grain in 5-inch x 40-Inch Motor	26
Fig. 12	Comparative Wave Form for (a) Typical Composite Propellant (PBAN 103), and (b) Nitrasol Propellant (NIT 101).	28
Fig. 13	Plot of Time to Explosion vs. Surface Temperature For a Double Base Propellant	32

LIST OF ILLUSTRATIONS (Concl'd)

Fig. 14	Plot of Time to Explosion vs. Surface Temperature for an Aluminized Composite Propellant.	32
Fig. 15	Plot of Time to Explosion vs. Surface Temperature for Ammonium Perchlorate.	33
Fig. 16	Predicted Surface Temperature--Pressure Relationship (Powling and Smith data).	36
Fig. 17	Correlation of Threshold Pressure with $r_T T^*$	38
Fig. 18	Correlation of Threshold Pressure with $\rho_S T^*$, r_T and c	40
Fig. A-1	Particle Size Distribution for Ammonium Perchlorate	A-3
Fig. A-2	Particle Size Distribution for Potassium Perchlorate.	A-4
Fig. A-3	Particle Size Distribution for Typical Bimodal Blend of Ammonium Perchlorate	A-4
Fig. A-4	Particle Size Distribution for Typical Trimodal Blend of Ammonium Perchlorate	A-5
Fig. A-5	Particle Size Distribution for Bimodal Blend of Ammonium and Potassium Perchlorates	A-6

LIST OF TABLES

Table I	Experimental Propellant Formulations Containing Ammonium Perchlorate.	12
Table II	Propellant Formulations with Oxidizers Other Than AP. .	13
Table III	Axial Instability Test Data for Ammonium Perchlorate-Containing Propellants	16
Table IV	Occurrence of Transverse Mode Instability	24
Table V	Chamber Pressure Data for Transition from Stable to Unstable Operation for Motors with Rectangular Perforations	27
Table VI	Comparison of Threshold Pressure with Ballistic Parameters.	41
Table B-1	Summarized Results.	B-3
Table B-2	Specific Acoustic Admittance.	B-3

I INTRODUCTION

The incidence of combustion instability in solid propellant rocket motors has been the subject of many investigations since World War II. It was first observed in the extruded double base propellant rocket motors developed during the Second World War. Workers in the United States and Britain early recognized the problem as a resonance phenomenon associated with both acoustical waves and gas flow in the chamber. In the absence of a clear understanding of the exact coupling mechanism between the burning propellant and the gas phase oscillations, palliatives for the problem were usually sought. Thus holes were drilled in the naked tubular charges used in early rockets;¹ resonance rods later became a common panacea for the secondary peaks frequently observed with internally perforated cartridge-loaded double base grains.²

While early work might appear to have centered on double base propellants, the early composite propellants (the resin-bonded and polysulfide-based formulations) also experienced instability problems; these were usually overcome by minor formulation change. Improved instrumentation enabled most instances of instability to be related to the driving of relatively large amplitude, high frequency, transverse acoustic type oscillations. It was found, most fortunately, that the addition of aluminum proposed originally for increasing the specific impulse of propellants also created a working fluid in which the normally occurring high frequency transverse modes of instability were suppressed.*

Many workers over the years have developed useful qualitative correlations between combustion phenomena and certain properties of the propellant or the rocket motor. Several attempts have been made to correlate instability behavior with oscillatory heat transfer in the solid phase.³⁻⁵ In this case the resulting time lag induced

* This may not be necessarily true for very large motors.

in the propellant mass burning rate was able to sustain oscillatory waves.* Likewise, time lags in the diffusion and mixing of the oxidizer and fuel components could be responsible for instability. No comprehensive correlation of these theories with experiment has yet been attempted.

Studies on composite propellants also revealed a correlation between erosive burning and observed axial mode instability trends. The most unstable propellant of a series was found to be the one in which burning was most strongly augmented by tangential gas flow.⁵ This suggested that the two types of behavior were related to the same physical and chemical processes occurring at or near the surface of the burning propellant. These can be related to enhanced mixing in the diffusion flame at the surface, or increased heat transfer to the solid phase which may be augmented by self-heating reactions in the solid phase. It should be noted that the erosive burning concept has been studied in theoretical treatments⁶ and there appears to be no major problem which would cause it to be rejected as a very satisfactory explanation for the observed axial mode instability phenomenon.

With strong agreement between theory and practice, it was concluded that a study of 'erosive coupled' instability was in order. There appeared good promise that the improved experimental techniques used in work previously mentioned, combined with a study of a very wide range of propellants, could considerably enhance the correlations hitherto reported.

The work covered in this report has been principally carried out using a small rocket motor (40 pounds of propellant); typical high energy propellants have been investigated over the pressure range 300 to 3000 psi. Definite correlations for ammonium perchlorate-based propellants have been established between combustion instability in the axial mode and two main operational parameters, burning rate and motor pressure. Information has also been obtained on the role compositional factors such as catalysts

* Of course, this may well be modified by reactions in the subsurface layer.

and other oxidizers play in controlling stability. Transverse instability was also observed under certain conditions but no data correlation on this phenomenon has yet been found; perhaps its coupling mechanism is associated with different processes.

The experimental data correlation found has been examined in relation to several theories proposed as a means of explaining the driving of large amplitude, gas phase disturbances by the burning propellant surface. At present it does appear that a model based on the characteristic times associated with combustion within the granular diffusion flame* can explain the dependence of stability on chamber pressure and burning rate.

It is not considered that the time lag theory, as such, is completely proven since the correlation of our data has automatically suggested other rather specific tests of our tentative explanation. We propose to continue to study other propellant types; we will attempt to see if a lower stability bound exists and whether any other theoretical parameter, e.g. frequency, can be correlated with experiment.

In the body of the report, terms such as "stability" or "instability" will generally be used to refer to disturbances in the axial mode; occasional deviations from this use will be evident from the context.

* This concept developed by Summerfield seems to satisfactorily explain the steady state dependence of burning rate on pressure and thus appears a valid premise to build upon.

II RESEARCH OBJECTIVES

The ultimate objective of this research is to identify the chemical and physical processes responsible for unstable combustion during the burning of solid propellants in rocket motors. The principal specific goal is the understanding of erosive-velocity-coupled instabilities, primarily through the study of finite-amplitude axial instability.

A second specific goal is to provide comprehensive data for use by rocket design engineers in choosing propellants and associated grain configurations for particular applications.

III EXPERIMENTAL PROGRAM

Experimental Method

General

Our main experimental approach has been based on the pulse triggering of instability, previously reported by one of the authors^{7,8} and now used in both solid and liquid propellant rocket engines.⁹

The method is particularly adapted to the investigation of axial-mode instability. Although the pulse source may be modified to trigger disturbances of almost any initial amplitude, in the present work the emphasis has been on the investigation of finite-amplitude instabilities, with a nominal trigger pulse of 100 psi.

There are several reasons for the investigation of finite-amplitude instability. The most important from a practical standpoint is the possibility that a particular motor may be stable to small perturbations arising from general combustion noise but may be triggered into instability by events like the exposure of minor flaws in the propellant grain or the ejection of objects through the nozzle. It is worth noting that for axial-mode instability, finite-amplitude effects can become significant for relatively small perturbations. This arises from the fact, first pointed out by Hart et al., that, for instabilities which depend on velocity perturbations, the mean axial mass velocity in the grain port is a significant reference velocity.

Propellants having a stable region of operation at low pressure in a particular combustor may become incipiently unstable at higher pressures. There exists thus an instability threshold, characterized primarily by a threshold pressure, P_T , and a threshold linear burning rate, r_T ; in our studies a relatively large geometric scale was chosen since previous work^{10,11} indicated that the threshold would be only weakly dependent on grain parameters.

The actual threshold point was detected by careful bracketing using a carefully programmed multi-phase unit. The restriction ratio, K_n , for both stable and unstable operation was computed from the operation parameters and plotted against pressure, the intersection of the two restriction ratio plots being designated as the instability threshold. The method is shown graphically in Fig. 1.

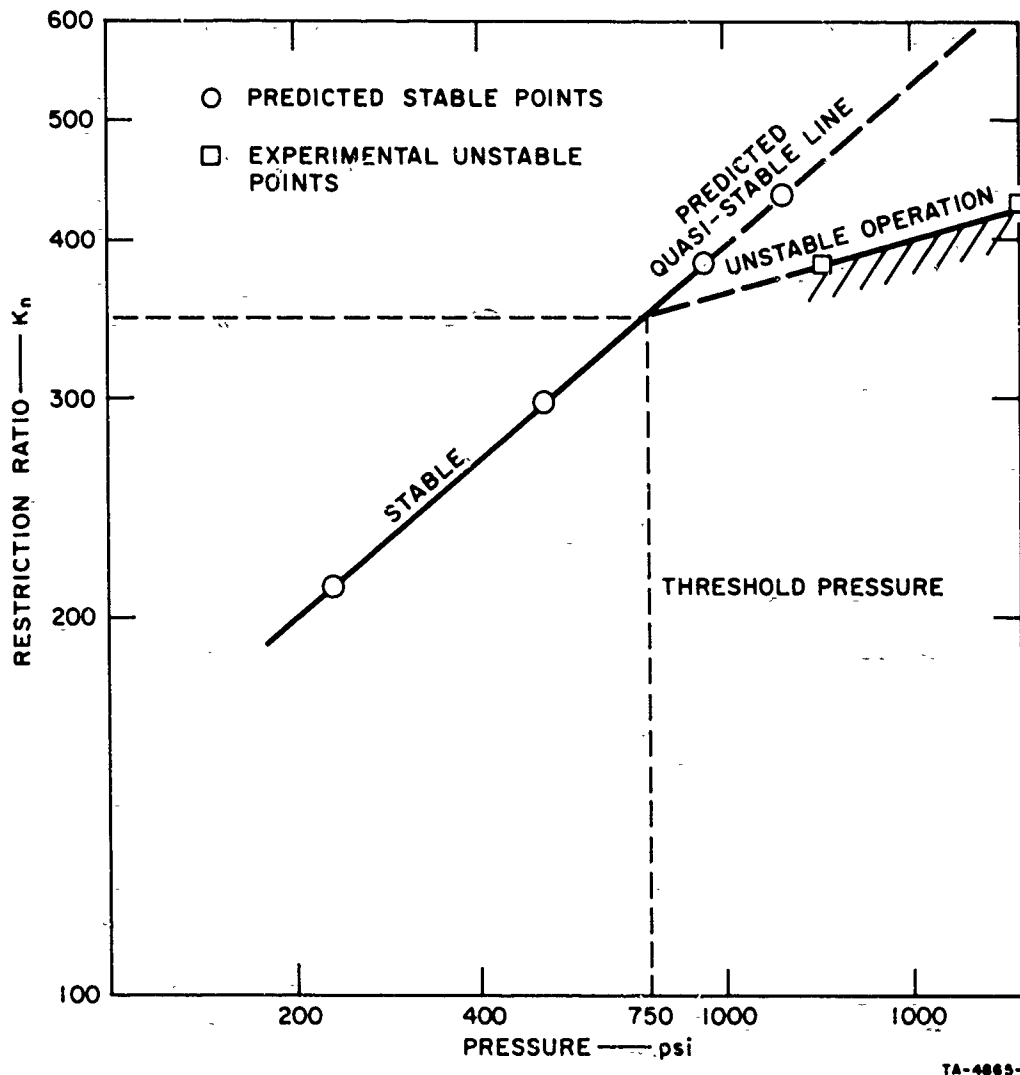


FIG. 1 SELECTION OF THRESHOLD POINT, BY EXTRAPOLATING UNSTABLE DATA POINTS BACK TO STABLE " K_n vs. P " PLOT
(Threshold burning rate obtained from associated burning rate data)

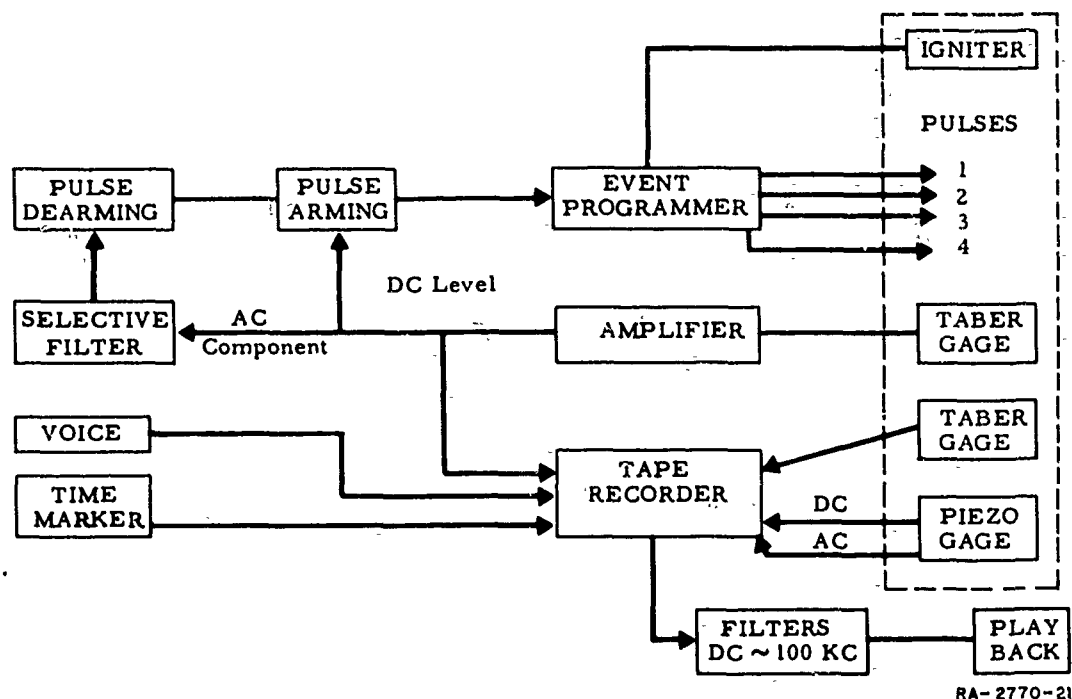


FIG. 2 INSTRUMENTATION BLOCK DIAGRAM

Test Instrumentation

Automatic programming of all firings was carried out using the programmer and instrumentation outlined in Fig. 2. The programmer, in addition to firing the igniter and pulses in correct sequence, incorporates an arming switch which is activated only by the output of a pressure transducer which monitors the chamber pressure. Consequently, no pulse can be fired unless the rocket motor is operating at the desired pressure. The programmer is also used to start the high speed camera at the prescribed time in the countdown in tests involving the window motor.

Steady state pressures were recorded in analog form on an oscillograph and on magnetic tape. The transducers used for this measurement were of the strain gage type (Taber); the frequency response of the combination used was approximately 500 cps.

For the measurement of the dynamic pressures (instability) a piezoelectric type transducer (Kistler) was used. The frequency response of

this latter transducer was limited by the type of adaptor used to couple it to the rocket chamber. Since the transducer is sensitive to heat, a water-cooled adaptor was necessary to alleviate the effects of the high heat flux encountered during unstable combustion. With the adaptor used, the frequency response was limited to 10 kc. Frequencies higher than this could be detected but the amplitudes of such frequencies could not be accurately determined. The output from the piezoelectric transducer was recorded on magnetic tape. For an analog record it was recorded on an FM track and for frequency analysis it was AC-coupled to a record track. The tape signal was re-recorded on an oscilloscope or oscillograph (through a variable band-pass filter, when necessary).

Rocket Motor Configurations

Static firings of the various propellants were carried out in a 5-inch-diameter by 40-inch-long chamber. Attached to the chamber were a multi-unit pulse head and a uniquely designed aft closure which houses the rocket nozzle, and a pressure relief device for over-pressure protection of the rocket chamber. This assembly is shown in Fig. 3. The size of this motor was selected to minimize scaling effects when comparing data from previous work.

During the early phases of the program, tubular grains were principally test fired since their progressively increasing pressure-time characteristic was desirable (significantly reducing the number of rounds needed to bracket the threshold pressure of a particular propellant). The pulses would generally be initiated at equal time intervals over the firing duration; as the data pattern evolved, very close bracketing of the threshold could be achieved.

Later in the program, rectangular or slotted grains were tested to study the damping effect of inert walls on axial instability. These motors were nozzled for an initial pressure above the threshold pressure and were driven unstable soon after ignition. As the operating pressure decreased and the inert wall area increased, the motors became stable.

The third type of motor utilized on this program was an opposed-slab grains with lucite sides. The so-called "window" motor was used for

NOTES:

1. REMOVE ALL BURRS AND BREAK SHARP EDGES APPROX. .0100.
2. GENERAL FINISH ∇ , EXCEPT AS NOTED.

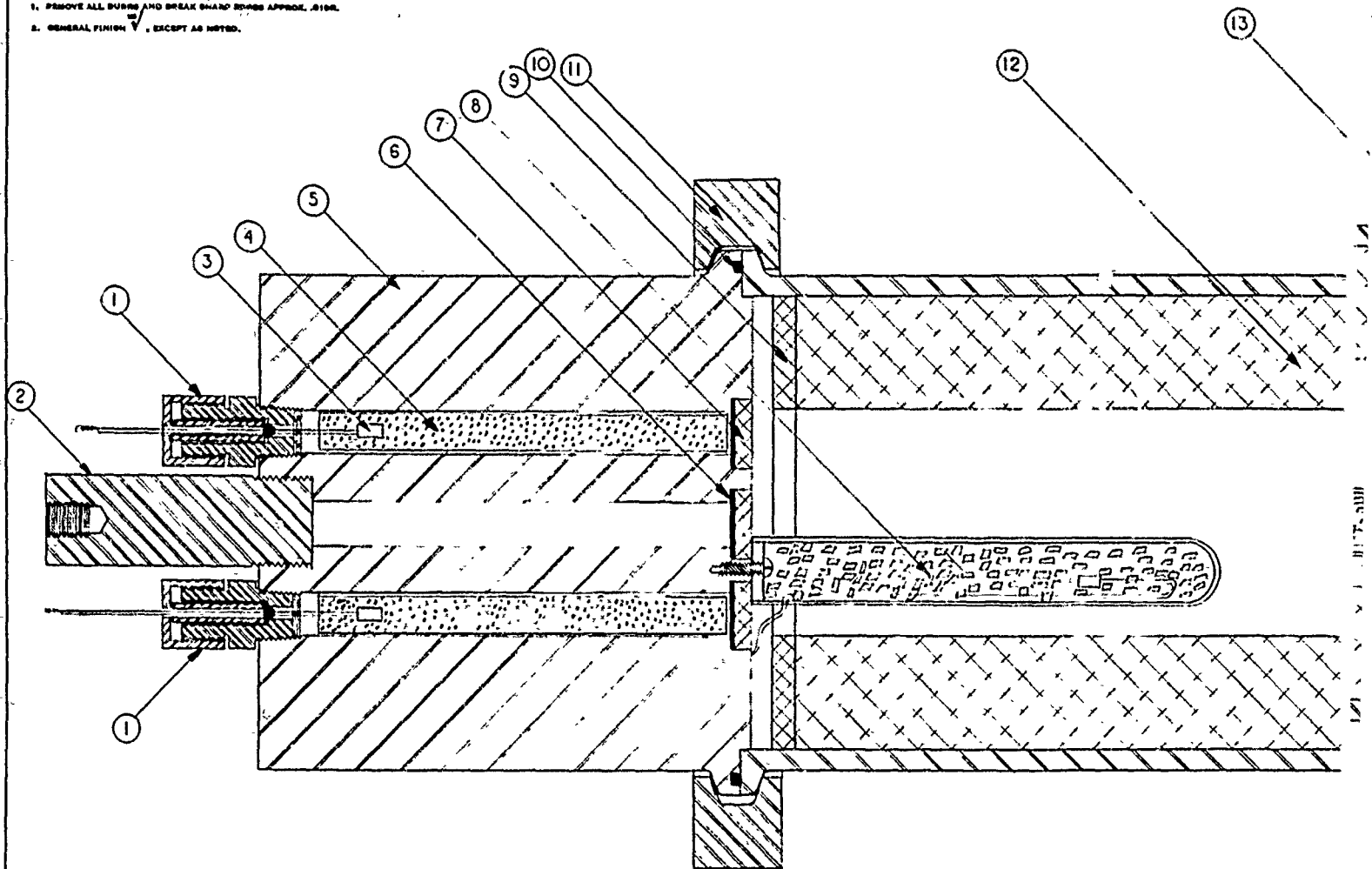
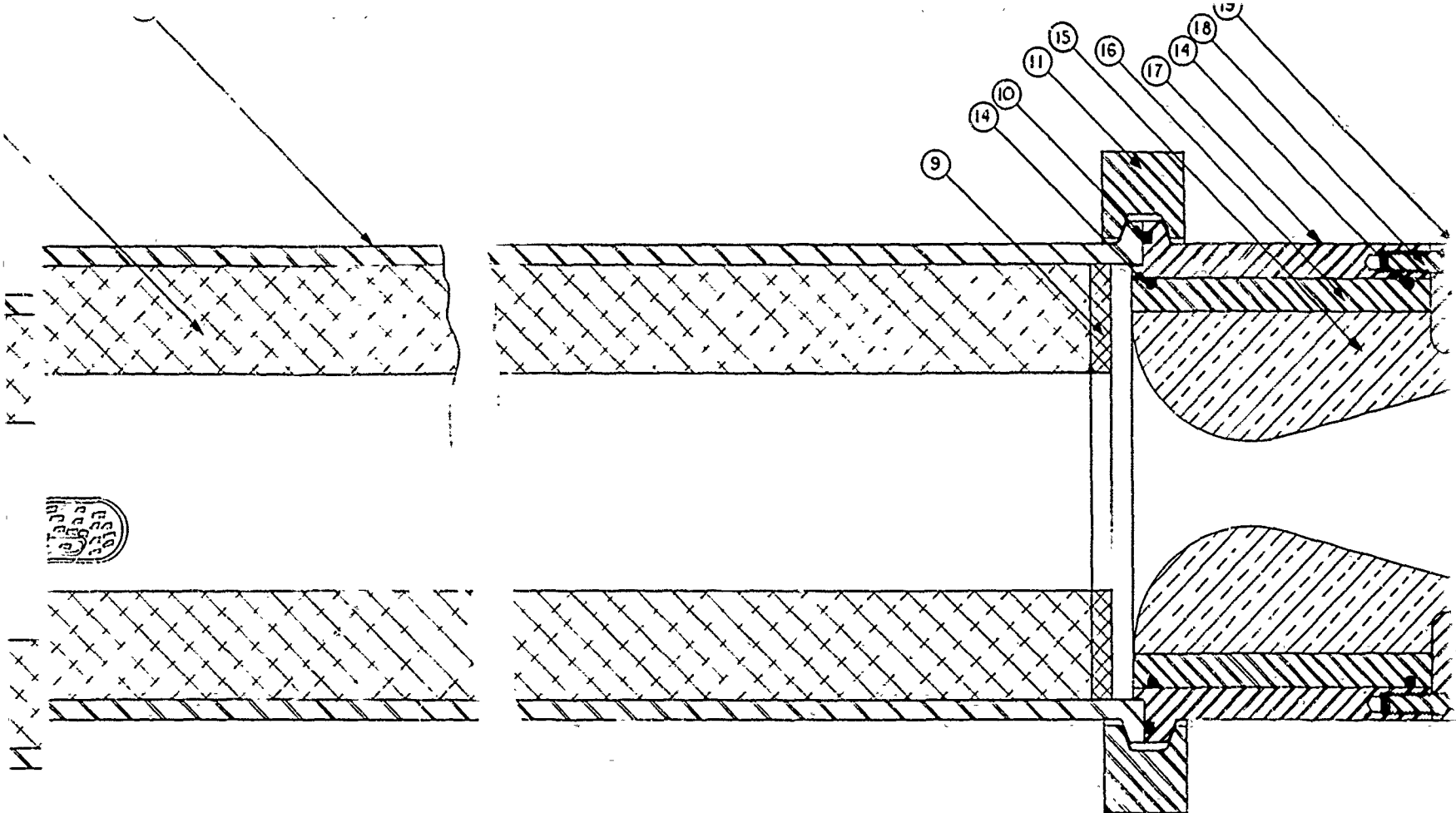


FIG. 3 5-INCH × 40-INCH



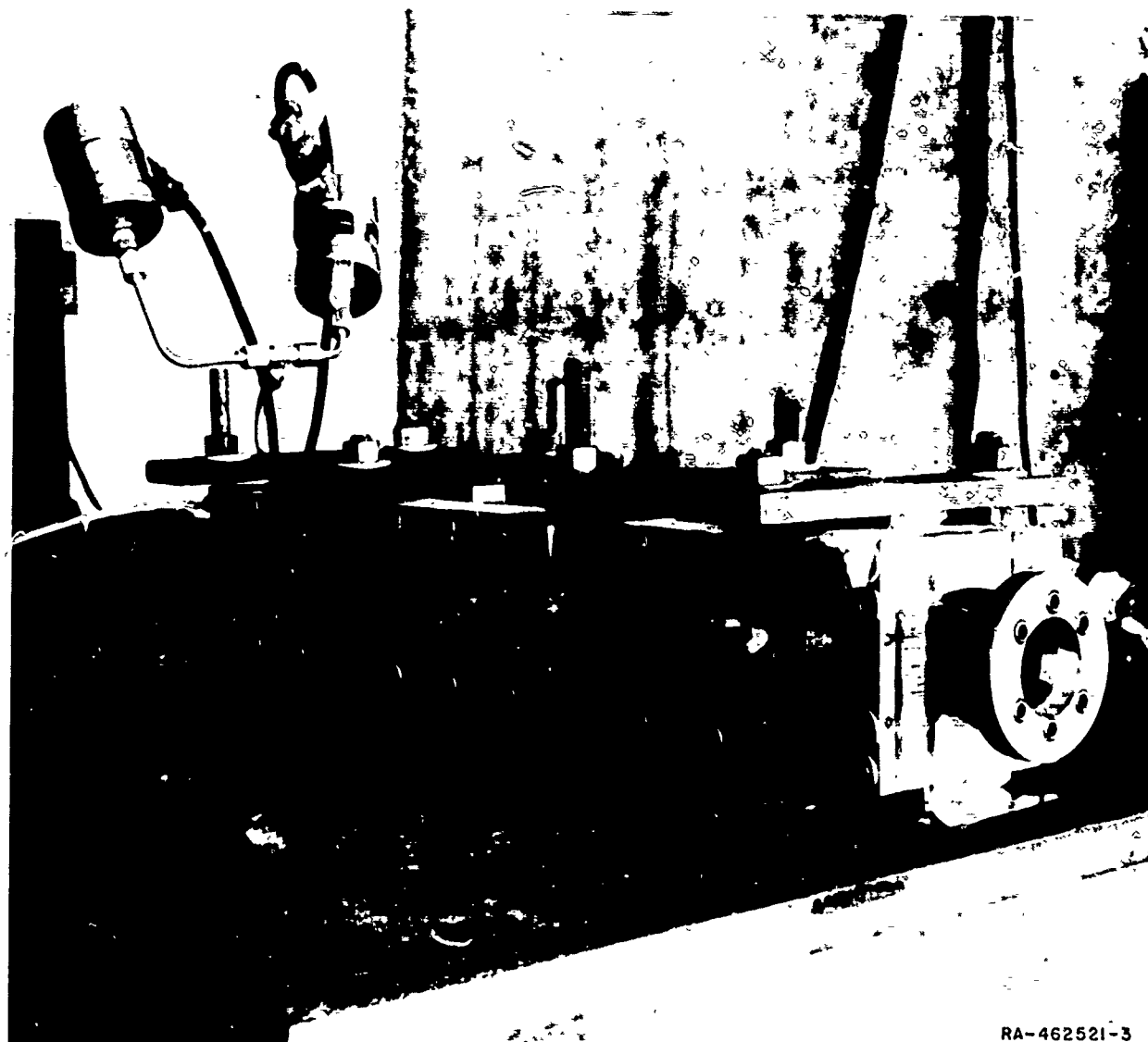
19	SRI	B-417	NOZZLE
18	SRI	C-411	SAFETY
17	SRI	C-412	NOZZLE
16	SRI	B-416	NOZZLE
15	SRI	B-416	NATICK 463T GE NOZZLE
14			PARKER
13	SRI	C-4	5 X 40
12			CASE B
11	SRI	D 410	HEAVY
10			PARKER
9			PROPEL
8			SRI BOP
7			POLY-A
6			.005 CC
5	SRI	C-434	MULTIPLE
4			5 GRAM
3			FFG BL
2			DUPON
1			MC TOR
			CONAX

DATE:	12/18/63	REVISION:	1
DESIGN:		APPROVED:	
BY:		DATE:	
APP:		TIME:	5" X 40"
APP:		MOTOR	
STANFORD RESEARCH INSTITUT			
MENLO PARK, CALIF.			

CH x 40-INCH UNSTABLE COMBUSTION MOTOR ASSEMBLY

CH

photographic studies of the combustion processes. Two different sizes-- 4 inch by 30 inch, and 2 inch by 20 inch--were tested; a typical motor is shown in Fig. 4.



RA-462521-3

FIG. 4 EXPERIMENTAL 2-INCH \times 20-INCH WINDOW MOTOR

Propellants Investigated

In order to gather data which would be directly applicable to present day problems, the propellants investigated in this program were, for the most part, typical of high performance state-of-the-art aerospace propellants.

Typical compositional factors studied include:

- a) aluminum and oxidizer particle size
- b) inclusion of burning rate catalysts and fast burning oxidizer
- c) binder type.

To study the role oxidizers play in modifying combustion response, propellants based on potassium perchlorate, lithium perchlorate, and ammonium nitrate were investigated.

The majority of the propellants studied were conventional composites; a preliminary study was also made on a system in which a nitrocellulose propellant base was loaded with an inorganic oxidizer and aluminum metal.

The actual compositions which were selected for study were originally chosen to encompass major compositional and ballistic changes. The propellants tested in this program are detailed in Tables I and II. The experimental results to be detailed later in this report will suggest, to the critical reader, other formulations which may be used to check certain aspects of the proposed combustion models. (It is proposed in future work to bridge the burning rate gap between the ammonium perchlorate and ammonium nitrate propellants.)

It should be noted that many propellants were formulated to support this study; Table I includes those propellants which could be safely mixed and loaded into the test motors or combustors. The propellants with a high fraction of fine oxidizer were cast only with difficulty using a displacement casting technique. Prior to large scale mixing, all the propellants were mixed in small batches to obtain mix v. density data and strand burning ballistic data.

Particular mention must be made of the problem of formulating propellants from unusual oxidizers. For instance, with potassium perchlorate all attempts to modify the burning rate by the inclusion of either combustion catalysts such as Fe_2O_3 or the endothermic burning rate depressant LiF failed to change the burning rate. These data suggest

Table I

EXPERIMENTAL PROPELLANT FORMULATIONS CONTAINING AMMONIUM PERCHLORATE
(Amounts in Wt. %)

Formulation No.	NH ₄ ClO ₄		KClO ₄		Catalyst	Aluminum ³	Binder ²
	Ground ¹	Unground	Ground	Unground			
102	24.0	44.2			1.5 LiF 1.5 LiF 1.0 Fe ₂ O ₃ 2.0 Fe ₂ O ₃ 2.0 Fe ₂ O ₃	15 Re 1131	PBAN, 16.8
103	24.0	56.0					PBAN, 20.0
104	22.5	56.0				15 Re 1131	PBAN, 20.0
105	22.5	44.2				15 Re 1131	PBAN, 16.8
106	23.0	44.2				15 Re 1131	PBAN, 16.8
110	23.0	44.2			0.5 Fe ₂ O ₃		PBAN, 15.8
111	22.0	56.0					PBAN, 20.0
159	12.0	28.0	12	28			PBAN, 20
161	{ 17.05 at 20μ 17.05 at 600μ	34.1				15 Re 1131	PBAN, 16.8
162	24.0	44.2				15 VM H322	PBAN, 16.8
166		60.0	20.0		0.5 Fe ₂ O ₃		PBAN, 20
170	23.5	44.2				15 VM H322	PBAN, 16.8
172	10.0	60.0	10.0				PBAN, 20
184	{ 17.05 at 20μ 17.05 at 600μ	34.1				15 VM H322	PBAN, 16.8
185	20	20 at 600μ		40			PBAN, 20
186	{ 20.0 at 20μ 20.0 at 600μ	40.0					PBAN, 20
189 M	60						PBAN, 20
108	22.5	52.5		20			PU, 25

¹ Average particle diameter of 10μ unless specified otherwise

² PBAN = polybutadiene, acrylic acid, acrylonitrile cured with epoxy

PU = polyurethane

³ Re = Reynolds

VM = Valley Metallurgical

Table II
PROPELLANT FORMULATIONS WITH OXIDIZERS OTHER THAN AP
(Amounts in Wt. %)

Formulation No.	Oxidizer			Aluminum	Catalyst	Binder
	Type	Ground	Unground			
NIT 101	AP	14	21	15 VMH 322		50 Nitro-cellulose binder
PBAN 109	KP	24.0	56.0	----		20.0 PBAN
PS 104	LP	22.02	51.38	----	0.97 Carbon	25.6 Poly-sulfide
PU 113	AN	16.5	47.5	10 VMH 322	1.0 Milori Blue	25 Poly-urethane

that the oxidation reduction reaction between organic reducing agents and KClO_4 , or its decomposition intermediates, is rate-controlling.

The ammonium nitrate and lithium perchlorate-based propellants posed severe formulating problems which were successfully overcome.

IV EXPERIMENTAL RESULTS

The experimental study performed was designed to obtain data on the role that compositional factors play in the incidence of combustion instability in rocket motors and to gain an insight into the fluid dynamic interactions between the combustion products and the burning propellant surface. Compositional factors, along with the related ballistic characteristics, were investigated using the 5-inch-diameter by 40-inch-long rocket motor; other studies were made using the window motors.

Data on Compositional Factors Study

It will be recalled from a study of Table I that the program was based primarily on a family of propellants derived from a propellant containing 80% ammonium perchlorate and 20% polybutadiene-acrylic acid-acrylonitrile terpolymer.

Compositional variations included burning rate control by inclusion of combustion catalysts, oxidizer particle size variation, aluminum addition, and change in oxidizer type. Limited studies were made in which the binder type was varied.

Ammonium Perchlorate-Based Propellants

The procedure outlined previously was used to study the instability characteristics of the various propellants. Typical pressure-time curves for one propellant, PBAN 162, triggered into instability at both high and low port-to-throat ratios, are shown in Figs. 5a and 5b. The instability data for the ammonium perchlorate propellants are detailed in Table III, the data cross plots for the propellants which could be triggered into instability are shown in Fig. 6.*

*The principal deviations from the straight line correlation shown in Fig. 6 occur for two propellants--PBAN 106 and PBAN 170. These deviations might perhaps be a result of a change in combustion mechanism at about 1000 psi or might be occasioned by variability in the black powder pulse characteristics. These possibilities will be investigated in future work.

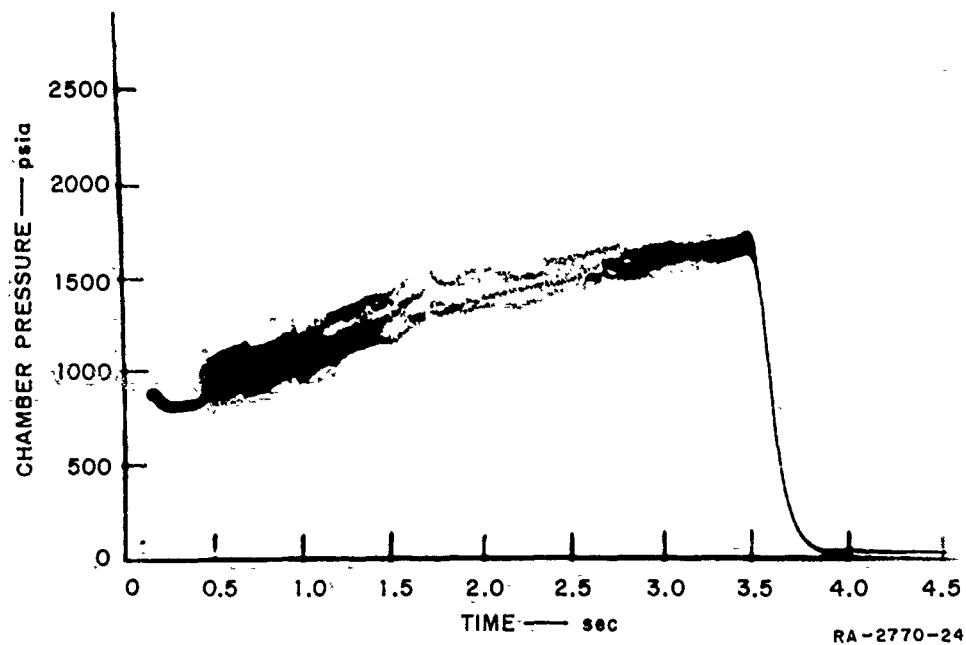


FIG. 5(a) INITIATION OF INSTABILITY ON INITIAL PULSE
(5-inch \times 40-inch motor composition PBAN 162)

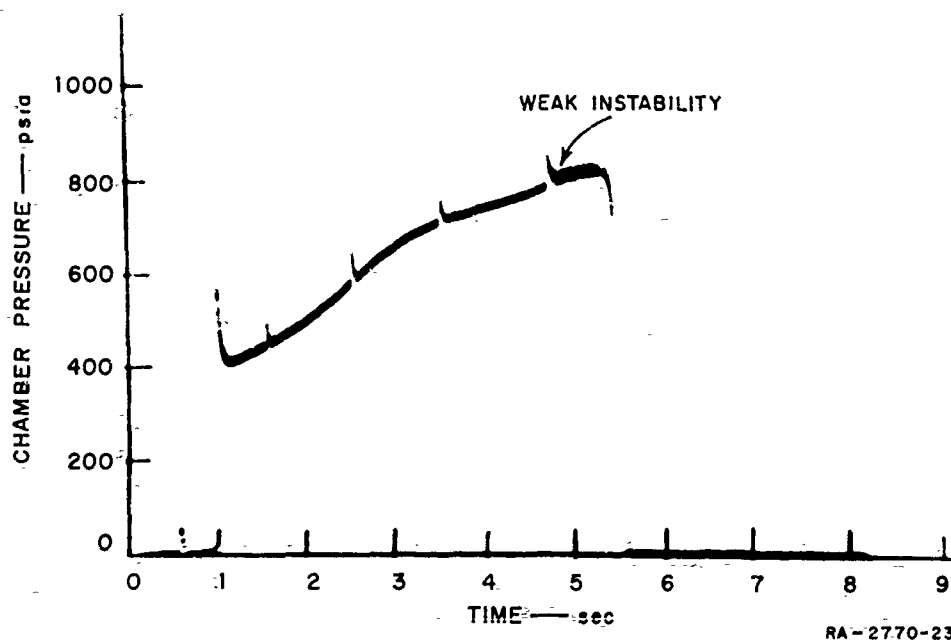


FIG. 5(b) INITIATION OF INSTABILITY ON TERMINAL PULSE
(5-inch \times 40-inch motor composition PBAN 162)

Table III

AXIAL INSTABILITY TEST DATA
FOR AMMONIUM PERCHLORATE-CONTAINING PROPELLANTS

Unstable Propellants	Threshold Data					
	Pressure, P_T , psia	Burning Rate, r_T , in./sec	A_t , in. ²	D_p , in.	J	K_N
PBAN 102	950	.325	1.23	3.30	7.0	330
PBAN 103	700	.30*	1.28	3.30	6.6	320
PBAN 104	360	.17*	1.83	4.08	7.1	270
PBAN 105	900	.315	1.37	3.80	8.8	340
PBAN 106	1600	.56	1.47	3.78	8.7	350
PBAN 161	750	.275	1.19	2.50	5.0	300
PBAN 162	760	.29	1.84	2.51	4.9	290
PBAN 166	500	.215*	1.33	3.70	6.9	265
PBAN 170	1350	.50	1.59	4.01	8.1	310
PBAN 172	530	.24	1.59	3.37	5.7	270
PBAN 184	700	.260	1.24	3.14	6.5	300
PBAN 186	720	.28*	1.22	3.47	8.1	340
PU 108	400	.18	1.49	3.47	6.4	285
Stable Propellants						
PBAN 110	Stable over range (400 psi - 2500 psi)					
PBAN 111	Stable over range (400 psi - 2500 psi)					
PBAN 159	Stable over range (400 psi - 2500 psi)					
PBAN 185	Stable over range (400 psi - 2500 psi)					
PBAN 189*	Stable axially over range (400 psi - 2500 psi)					

* Transitioned to transverse mode

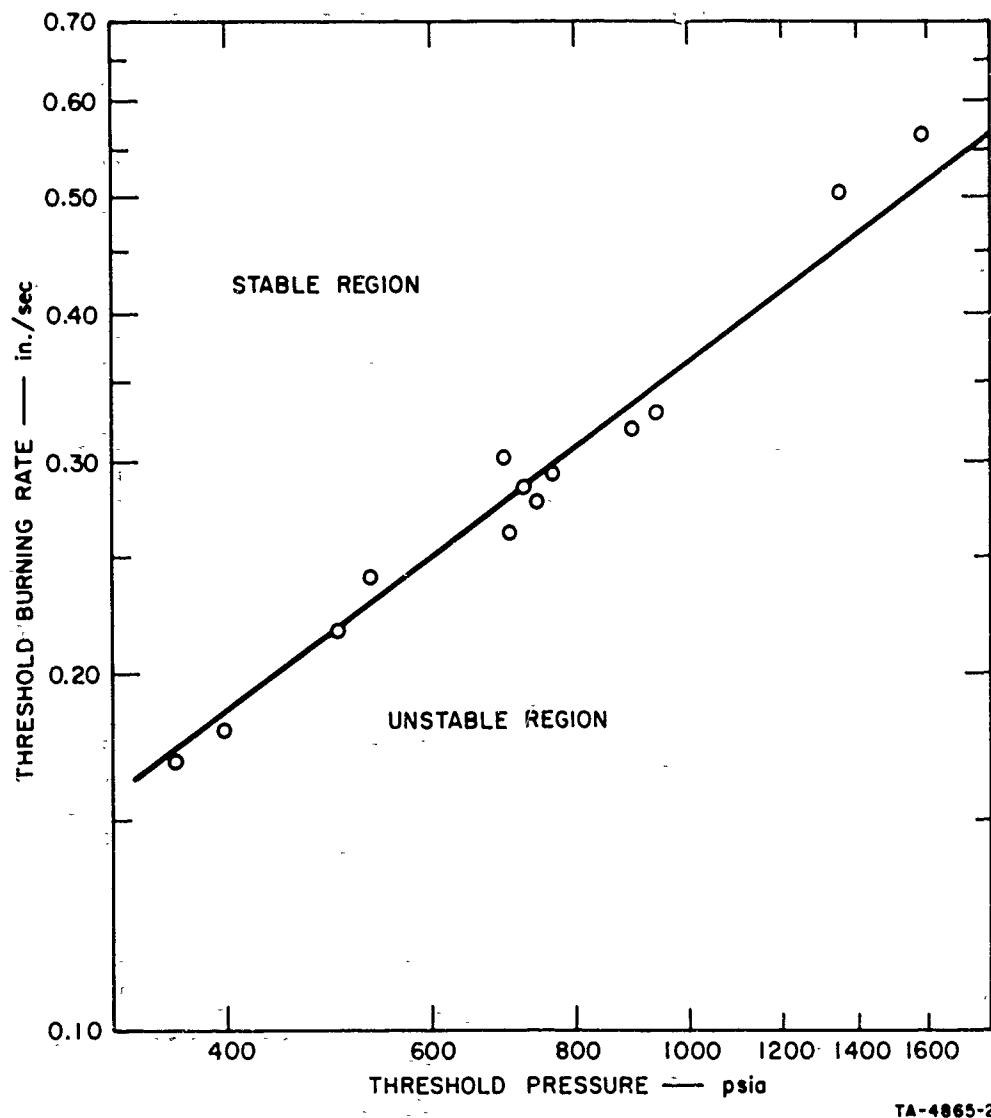


FIG. 6 CORRELATION OF THRESHOLD PRESSURE WITH PROPELLANT BURNING RATE 5-INCH \times 40-INCH ROCKET MOTOR

An examination of our data in Table III and Fig. 6 shows that most of the typical aerospace propellants sustain axial mode instability in our test motor; those propellants, particularly those including catalysts whose pressure-burning rate relationship lies above our stability boundary, will most probably not sustain axial disturbances at frequencies less than 500 cps. An examination of the data in Table III will permit cross plotting between ballistic parameters other than those correlated in Fig. 6; no relationship other than that between chamber pressure and burning rate has been found.

Principal Observations Relating to Ammonium Perchlorate-Based Propellants

Some general remarks on these data are in order:

<u>Factor</u>	<u>Observation</u>
Rate Deterrent - Lithium Fluoride	1) The addition of an endothermic burning rate catalyst, LiF, lowers the burning rate and thus aggravates combustion instability.
Rate Accelerant - Iron Oxide	2) The addition of a burning rate accelerator, Fe_2O_3 , enhances the burning rate and improves stability.
Aluminum	3) The addition of aluminum did not promote stability other than by its influence on burning rate.
Very Coarse Ammonium Perchlorate	4) The inclusion of a small fraction of extremely coarse ammonium perchlorate did not aggravate stability.
Potassium Perchlorate	5) The role of KClO_4 may be to improve stability through enhancement of burning rate.
Particle Size	6) The use of a very fine oxidizer increases burning rate and stability; fine aluminum powder enhanced the burning rate and stability more than coarse aluminum powder.
Transverse Instability	7) Regardless of burning rate, non-aluminized propellants transitioned, on occasion, to transverse mode instability.

Mixed Oxidizer Propellants

The very wide range of burning rate dependence on particle size distribution in a mixed oxidizer system based on ammonium perchlorate and potassium perchlorate enabled two propellants with identical thermochemistry but vastly different burning rates to be formulated.

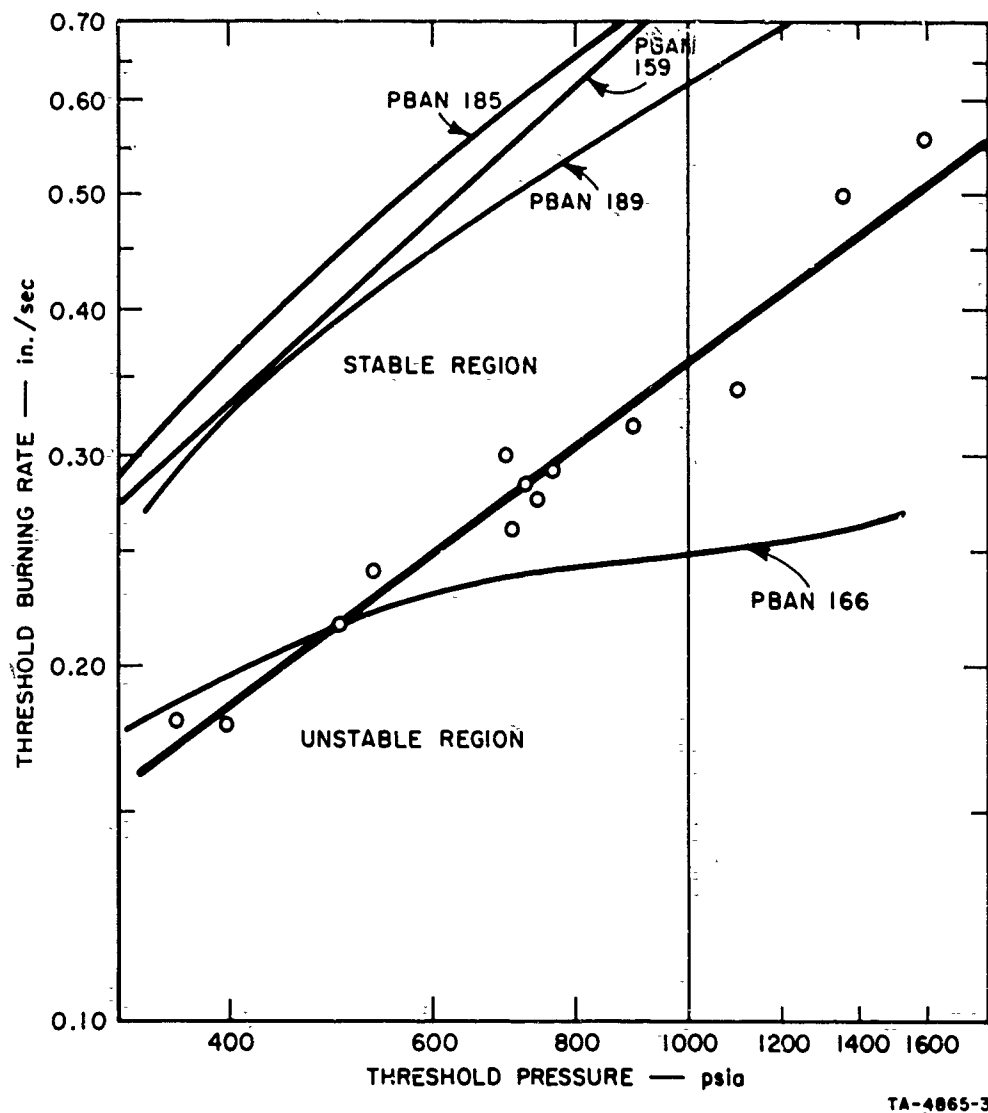


FIG. 7 THRESHOLD DATA FOR MIXED OXIDIZER PROPELLANTS

These two propellants, PBAN 166 and PBAN 189, were tested in our motor. The slow burning propellant could be driven unstable in the axial mode while the fast burning analog was stable. Both propellants were unstable in a high frequency, presumably transverse mode. The data for these propellants are shown in Fig. 7.

Two other mixed oxidizer propellants were formulated to ascertain if the use of very coarse ammonium perchlorate particles could result in unstable burning in a fast burning propellant. These propellants, PBAN 159 and PBAN 185, had very similar burning rate curves (Fig. 6) and were both stable to axially driven flow disturbances.

Propellants Based on Different Oxidizers

Over the years many observations have been recorded on the combustion characteristics of propellants based on potassium perchlorate, lithium perchlorate, and ammonium nitrate. The general tenor of reports has been that these propellants were stable; but this perhaps resulted from their limited use. We therefore decided to evaluate them in this program because it is known that metal salt oxidizers decompose by different processes than those of the fuel salts. A further point believed to be significant was that ammonium perchlorate sublimed during burning while the other oxidizers melted.

As mentioned earlier, considerable effort was devoted to developing slow burning potassium perchlorate propellants and fast burning ammonium nitrate propellants. This work, aimed at producing ballistic characteristics similar to those of the ammonium perchlorate propellants, was not successful. (Future work will include ammonium nitrate propellants modified with potassium perchlorate and ammonium perchlorate.)

The potassium and lithium perchlorate propellants were both stable when pulsed at pressures up to 2,500 psia. The ammonium nitrate propellant was also stable. While no instability was noted, an anomalous ballistic

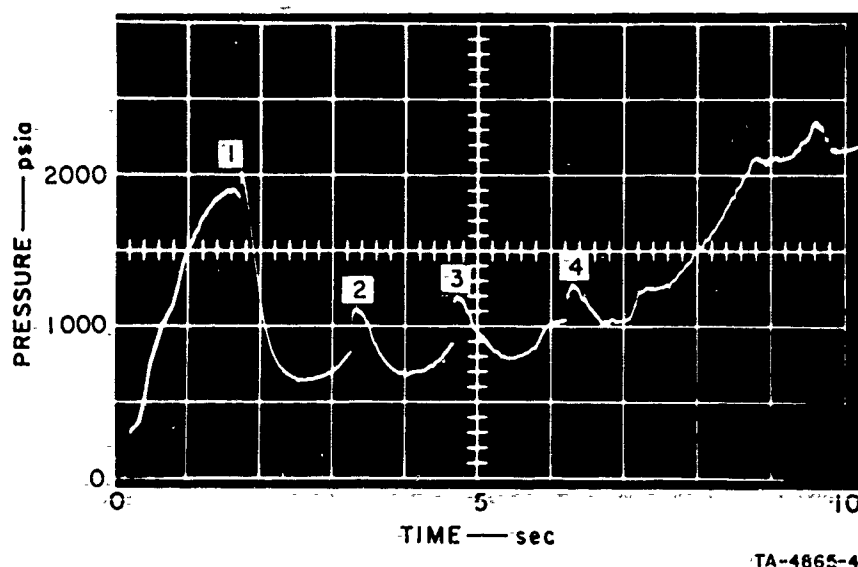


FIG. 8 FIRING RECORD FOR AMMONIUM NITRATE PROPELLANT GRAIN (first 2 seconds show burning of starter grain), PULSES AS CODED 1, 2, 3, AND 4

phenomenon was observed (Fig. 8). Following the firing of the trigger pulse there occurred a pressure hump which initially carried a 500 cps ripple. This ripple decayed and the pressure slowly fell back to the normal level. This phenomenon repeated itself on all four pulses and was duplicated exactly in two firings; after the fourth pulse, an unexplained pressure rise was observed. The burning rate data for these propellants, relative to typical ammonium perchlorate propellants, are shown in Fig. 8.

High Energy Double-Base Propellants

A composite modified double-base propellant was tested to investigate whether a high energy binder modified the response of the combustion processes to pulsing. The propellant used--NIT 101--contained aluminum (15%) and ammonium perchlorate and it possessed a very high flame temperature. The burning rate, shown in Fig. 9, was quite close to the stability bound found for the ammonium perchlorate composite propellant. One motor, when pulsed at a pressure close to 1900 psia, was stable, while another motor, pulsed at a lower pressure, went unstable at 1400 psia (see Fig. 10). Both motors transitioned to the transverse mode at high pressure, regardless of the fact that they contained 15% aluminum powder.

Transverse Instability and Associated Phenomena

While this investigation has been primarily concerned with axial instability in the intermediate frequency range, some very interesting observations have been achieved on other types of combustion phenomena. So far we have not been able unequivocally to identify the true nature of the other instabilities which are perhaps therefore best described as secondary peaks. In some cases a rapid increase in pressure has been associated with low-amplitude high-frequency oscillations characteristic of the natural transverse acoustical frequencies; in other cases the analysis of the head-end piezoelectric pressure transducer has not detected these characteristically high frequencies. This could be due to a complex wave pattern in the combustor, or to frequency limitations of the gage mount.

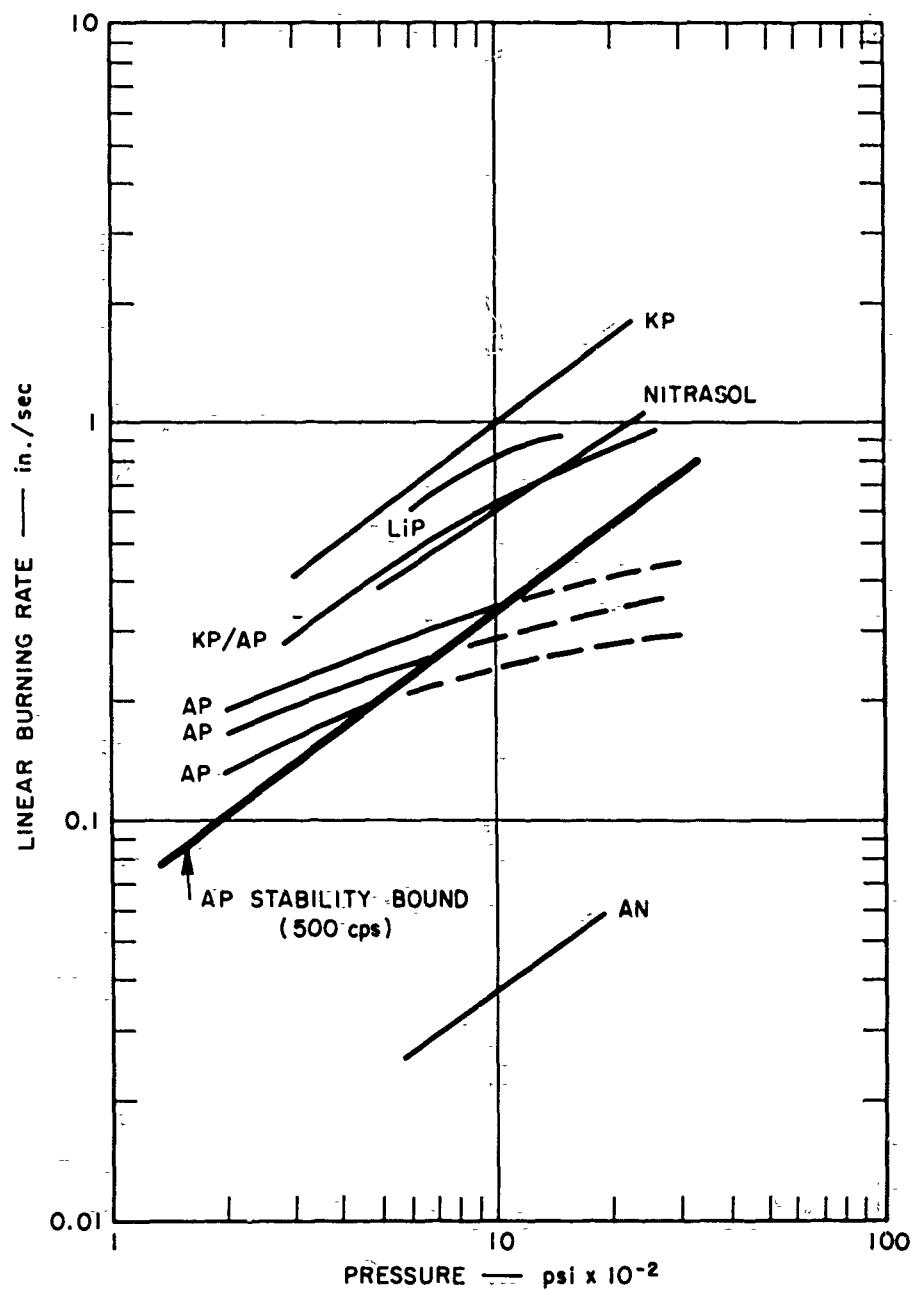


FIG. 9 TYPICAL PROPELLANT BURNING RATES; SOLID LINE STABLE REGIME, DOTTED LINE UNSTABLE REGIME FOR 5-INCH x 40-INCH MOTOR
Note: Aluminized-nitrasol propellant unstable in one firing

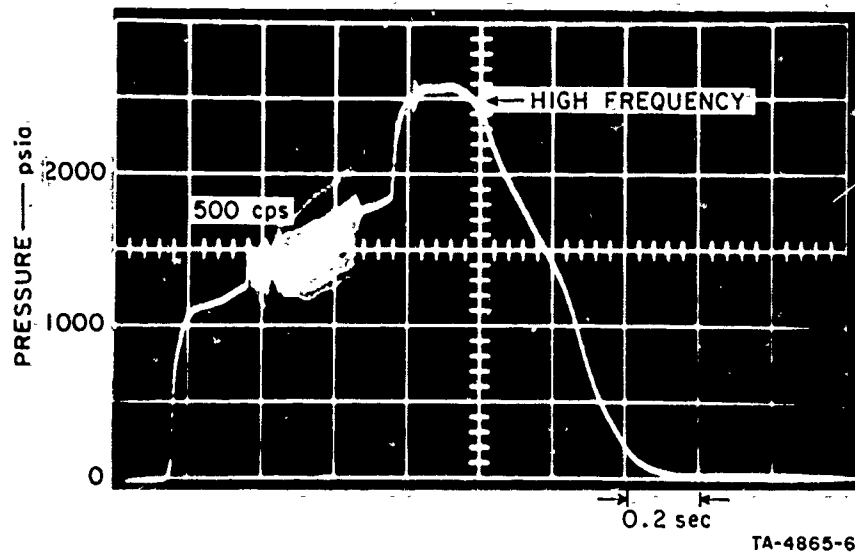


FIG. 10 ALUMINIZED NITRASOL PROPELLANT, NIT 101,
EXHIBITING FIRST AXIAL MODE (500 cps)
AND THEN A HIGH FREQUENCY INSTABILITY (>10 kc)

The secondary peaks we observed may possibly arise from vortex flow of the combustion products, the mass burning rate perhaps being augmented by both pressure and velocity-coupled processes. Another explanation might be the transverse/wave-coupled thermal explosion process in the solid phase induction zone (perhaps also associated with vortex flow).

Evidence for vortex flow rests on the work of Swithenbank and Sotter who convincingly explain the high tangential torques often observed in experimental firings; the spinning mode of instability could, under certain conditions, also explain the presence of the observed torques. The thermal explosion process appears to offer an alternative to other proposed methods of coupling as a driving mechanism for the high frequency type of instability. Further comments on these points will be made in the discussion of our results.

The experimental data concerning the incidence of transverse instability or secondary peaks in motors containing our experimental propellants are given in Table IV. It will be noted that it has occurred with most types of composite propellants that did not contain aluminum. No pattern of behavior was found to distinguish fast burning propellants from slow burning propellants as was observed for the intermediate frequency axial

612-174

instability. The amplitude of the chamber pressure was frequently extremely high and in most cases the pressure relief device operated. However, in some cases the excess pressure was held in the combustor and the pressure excursion decayed to the predicted pressure level. This latter behavior is in accord with experience observed over the years with double base and some composite propellants; usually a motor is prone to instability over certain discrete time periods during operation, presumably only when the driving processes characteristic of the burning propellant are correctly phased in relation to acoustical waves.

Table IV
OCCURRENCE OF TRANSVERSE MODE INSTABILITY

Propellant	Test No.	$P_{c \text{ TRAN}}$, psi	r_b in./sec	K_N	J	L_p/D_p
PBAN 103	14	990	0.28	330	7.40	11.17
PBAN 103	35	1455	0.302	464	14.35	8.09
PBAN 104	32	1485	0.240	466	13.91	8.37
PBAN 104	34	1085	0.230	466	19.74	5.90
PBAN 104	1	890	0.245	311	7.04	11.02
PBAN 104	2	615	0.260	309	9.56	8.01
PBAN 166	17	1090	0.250	385	12.42	7.75
PBAN 166	28	1415	0.265	446	14.21	7.83
PBAN 186	23	1030	0.31	390	9.76	9.97
PBAN 189	45	1415	0.81	226	4.56	12.40
PBAN 189	47	1365	0.79	236	4.99	11.86
NIT 101	57	2075	0.980	302	8.27	8.93
NIT 101	69	2040	0.970	247	5.69	10.84

Note: $P_{c \text{ TRAN}}$ = pressure at which motor transitioned from stable operation to a high frequency transverse mode of instability.

One fact to be noted is that the very high energy nitrasol propellant containing 15% by weight aluminum exhibited secondary peak behavior; this is unusual but may support an observation made by Trubridge* that increase in energy may stimulate instability. It should be noted that our experimental program was not originally concerned with high frequency instability, but it does appear that the differing characteristics of propellants in relation to the type of instability behavior may throw additional light on the driving processes available in a burning solid propellant.

Motor Dimensional Parameters and Combustion Instability

To verify our assumptions that the motor geometry selected was not operating on the borderline of a geometrical stability bound, a series of motors with varying length to diameter ratios was tested. Four motors, all five inches in diameter, with lengths of 15, 21, 31, and 40 inches were test fired with propellant PBAN 104. The 15 inch and 21 inch motors were stable at pressures of 790 and 690 psi respectively; the 31 inch motor went unstable at 370 psi, as did the 40 inch motor. The initial perforation diameter was 2.5 inches in all cases.

From these experiments it certainly appears that low length to diameter ratios favor stability as far as the axial mode of instability is concerned. It is not possible to generalize beyond this, since our study was not primarily aimed at low aspect ratio motors.

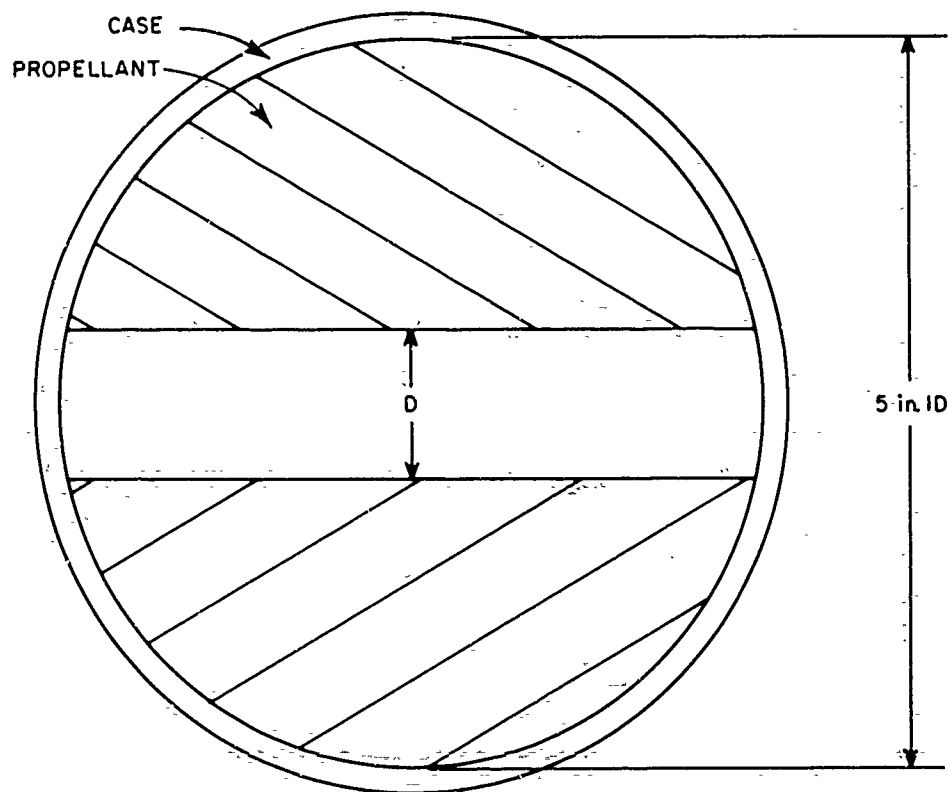
Motor geometry did to some extent affect the conduct of our tests; in order to obtain pulses of 100 psia amplitude it was necessary to increase the gunpowder charge as the throat area increased. Likewise in one instance at a pressure well above the threshold pressure it was observed that instability could be triggered using a smaller disturbing charge.

*Trubridge, G. P., Private communication, Imperial Metals Industry, Summerfield Research Station (England).

Grain Geometry Factors

Although the work is incomplete at this time, the pulsing studies using an opposed slab grain with a quasi-rectangular perforation in our 5 by 40 inch motor provides a motor variant with interesting possibilities (Fig. 11). In this motor the driving area (burning surface) decreases as the dampening area (side wall) increases. Thus, sometime during burning the losses sufficiently predominate that the instability dies out. Data from some preliminary experiments are given in Table V. For PBAN 104 the pressure at which instability ceases becomes lower as the ratio of burning surface area to dampening area increases. When another propellant was tested (PBAN 103), there appeared to be no correlation with the same data from PBAN 104.

A very interesting observation was made on the need for good acoustical symmetry if instability of burning is to occur. One motor containing PBAN 103 was test fired and found to be stable at pressures where previously the same propellant was unstable. The sole difference



D, PERFORATION WIDTH WAS EITHER 1.0 in. OR 1.75 in.

TA-4865-11

FIG. 11 OPPOSED SLAB GRAIN IN 5-INCH \times 40-INCH MOTOR

was that the opposed propellant surfaces were offset from the motor centerline; presumably the dampening in the cavity increased.

Table V

CHAMBER PRESSURE DATA FOR TRANSITION FROM STABLE TO UNSTABLE
OPERATION FOR MOTORS WITH RECTANGULAR PERFORATIONS

Propellant	Test No.	P_i , psi	$\frac{A_{Bd}}{A_{Dd}}$	P_d , psi	K_{nd}	r_d , in./sec
PBAN 104	51	1015	0.782	840	545	0.258
PBAN 104	55	785	0.867	540	325	0.240
PBAN 104	66	590	1.41	340	330	0.164
PBAN 103	64	1305	1.79	1165	500	0.291
PBAN 103	67	930	1.15	680	373	0.250

Note:

- P_i = Initial pressure level in motor prior to pulsing
- A_{Bd} = Burning surface area at transition point
- A_{Dd} = Dampening (inert) surface area at transition point
- P_d = Chamber pressure at transition to stable operation
- r_d = Propellant burning rate at transition to stable operation
- K_{nd} = Restriction ratio at transition point.

Window Motor Studies

A series of tests were made using our window motors, containing lithium fluoride catalyzed propellant, in an attempt to correlate high speed photographs of the wave motion in an unstable motor with piezo records of the pressure disturbances. With a 3 x 30-inch motor and a 1 inch perforation, we found that it could not be driven unstable at pressures well above the critical pressure found for the same propellant in a 5 x 31-inch radial-burning motor with a 2.5-inch perforation. Some pulse trains, however, lasted for periods up to 200 milliseconds before decaying. During this period the movies appear to show a standing wave

pattern set up within the motor. Our lack of success with this design prompted us to design a smaller motor capable of operation at higher pressures. This unit, 2 x 20 inch motor with an 0.5-inch perforation, also proved to be highly stable even though pulsed to 800 psi.

The inherent stability of the rectangular perforated motors has necessitated a new approach to this aspect of the problem.

Wave Phenomena

The characteristics of the pressure wave have been examined using the close coupled water-cooled piezoelectric transducer. All propellants containing ammonium perchlorate give a typical steep fronted pressure wave shown in Fig. 12a. The data for the double base propellants (Fig. 12b) show a pronounced initial sharp pulse which suggests perhaps a different burning rate response to the periodic pressure wave.

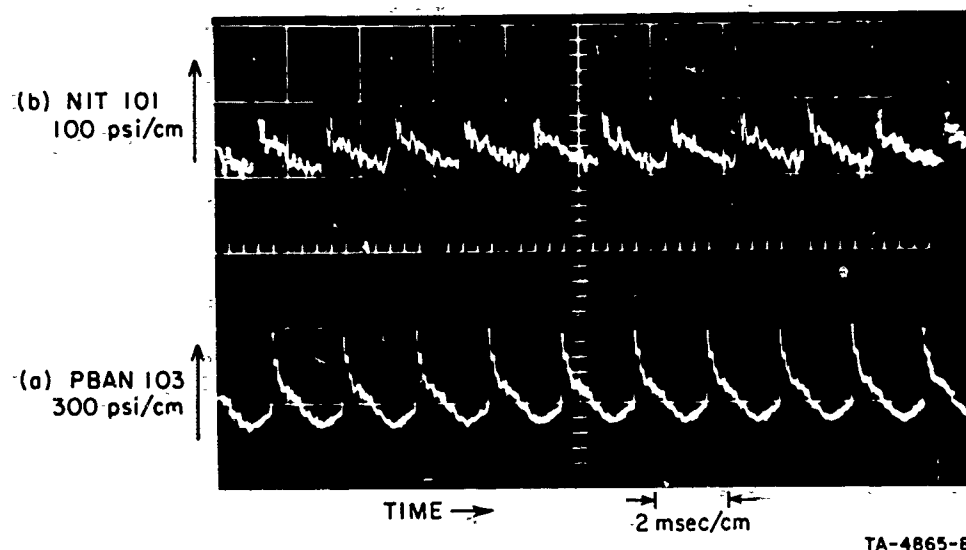


FIG. 12 COMPARATIVE WAVE FORM FOR (a) TYPICAL COMPOSITE PROPELLANT (PBAN 103), AND (b) NITRASOL PROPELLANT (NIT 101)

V DISCUSSION AND APPLICATION OF SIGNIFICANT RESEARCH FINDINGS

Our experimental correlation of instability data for a range of composite propellants has been examined in relation to two of the principal approaches used in understanding instability in large motors. These are (1) the approaches based on Crocco's¹³ time lag hypothesis which has been used successfully in interpretation of liquid engine combustion instability, and (2) the acoustical theory of Hart and McClure,¹⁴ which has provided a framework for studying the combustion instability of solid propellants. The latter theory has been successful in explaining many aspects of instability through a phenomenological approach in which a combustion zone is collapsed into a surface having an acoustical admittance. Our experimental study seeks to complement these general approaches by considering the chemical and physical processes (both solid and gas phase) occurring in the combustion zone.

The practical application of our data in relation to the design of rocket motors is discussed in the third part of this section.

Characteristic Combustion Time Relationship

In examining the phases of the combustion mechanism which could be concerned with instability buildup through the concept of critical lag time, we have for a composite propellant three possibilities:

- 1) Homogeneous gas phase reactions
- 2) The granular diffusion flame of Summerfield
- 3) Reactions in the subsurface induction zone; this could be manifested in one extreme by a thermal explosion or by cyclic variation in burning rate.

The homogeneous gas phase reactions do not immediately appear capable of explaining the more frequent occurrence of axial instability with composite propellants than is observed with double base propellants. The recent paper by Sirigano and Crocco¹⁵ suggests, however, that the gas phase reactions, once they can be clearly identified, should be closely

studied. The diffusion flame and subsurface reactions are attractive as the coupling processes, since they may have characteristic delay times which can act as the strong forcing function for the acoustical oscillations in the gas phase. It should also be noted that "erosive" coupled instability has been observed with many propellants for which pressure coupling is nonexistent; the diffusion flame is extremely sensitive to increased mixing induced by velocity fields.

While the granular diffusion model is particularly appropriate for composite propellants, subsurface reactions such as coherent triggered thermal explosions might be applicable mechanisms for both homogeneous double-base propellants and composite propellants. The conventional approach to this latter concept is that originated by Frank Kamenetsky.¹⁶

While it does not appear that our data on intermediate frequency instability are best interpreted on the basis of the thermal explosion concept, it will be presented here since it may, under certain circumstances, explain resonance phenomena (see for example, Clemmow and Huffington's treatment of Chuffing).¹⁷

Thermal Explosion Model

The approaches of Kamenetsky, as modified by others, notably Gray,¹⁸ can be used to develop a model for the surface zone. It may be postulated that the propellant burns by a series of local thermal explosions which are time-phased by an acoustical wave--the subsurface layer or induction zone being heated by an internal homogeneous or heterogeneous reaction, and burning proceeding by a series of thermal explosions rather than a steady state decomposition. Since the subsurface layer is heated by the normal heat flux from the combustion zone, periodic fluctuations in the pressure or velocity fields at the surface may result in periodic variations in the subsurface temperature of the layer.

Gray¹⁸ has reviewed the conditions for thermal explosion for homogeneous materials such as explosives, and Gross and Amster¹⁹ have cataloged the necessary parameters for several typical propellants. According to Gray the time required to reach a runaway reaction condition is:

$$t_2 = \frac{RT_0^2}{E} \cdot \frac{C}{QA} \cdot \exp \frac{E}{RT_0}$$

where E is the activation energy

C is the specific heat

Q is the heat of reaction.

It will be seen that E, C, and Q are characteristics of any given explosive material,* while A--the pre-exponential function--may be expected to vary with the degree of heterogeneity in a multi-component propellant and could vary with the catalyst content. In the classical treatment a film heat transfer coefficient of unity is assumed and hence T_0 is identified with the environmental temperature. In the case under study the effective film coefficient is much less than unity and it is probably more appropriate to identify T_0 as the surface temperature.

On the basis of Powling and Smith's data the surface temperature, T_0 , can be related to the pressure in the combustor; moreover, since the subsurface temperature profile is dependent on burning rate, T_0 may vary somewhat from the actual surface temperature.

An examination of the expected relationship of combustion lag times and the most critical parameter for the thermal explosion model, T_0 , does not suggest that this model can explain our experimental results.

Lack of agreement does not permit a total rejection of the thermal explosion model since it does appear to be capable of sustaining periodic pressure oscillations. To illustrate this point, the explosion times as a function of temperature have been computed for a double base propellant, an aluminized composite propellant, and pure ammonium perchlorate (see Figs. 13, 14 and 15). Surface temperatures in the range 600°K to 1200°K have been proposed for many propellants and it will be seen that a wide range of explosion times can be encompassed which are characteristic of wave frequencies from a few cps to 100 Kc or more. These could be

*

Note, however, C is a function of temperature.

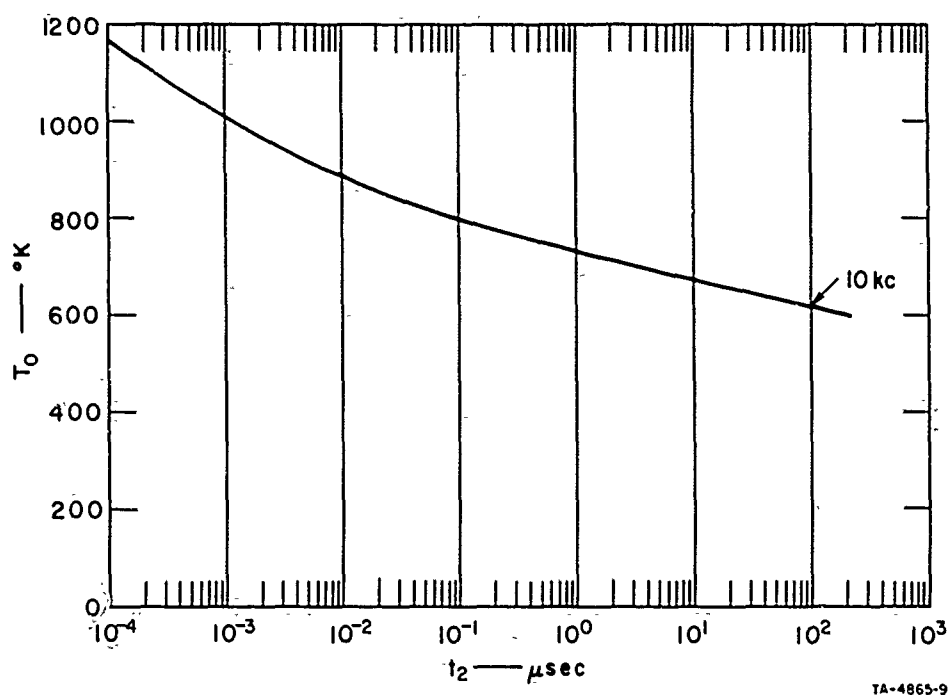


FIG. 13 PLOT OF TIME TO EXPLOSION vs. SURFACE TEMPERATURE FOR A DOUBLE BASE PROPELLANT

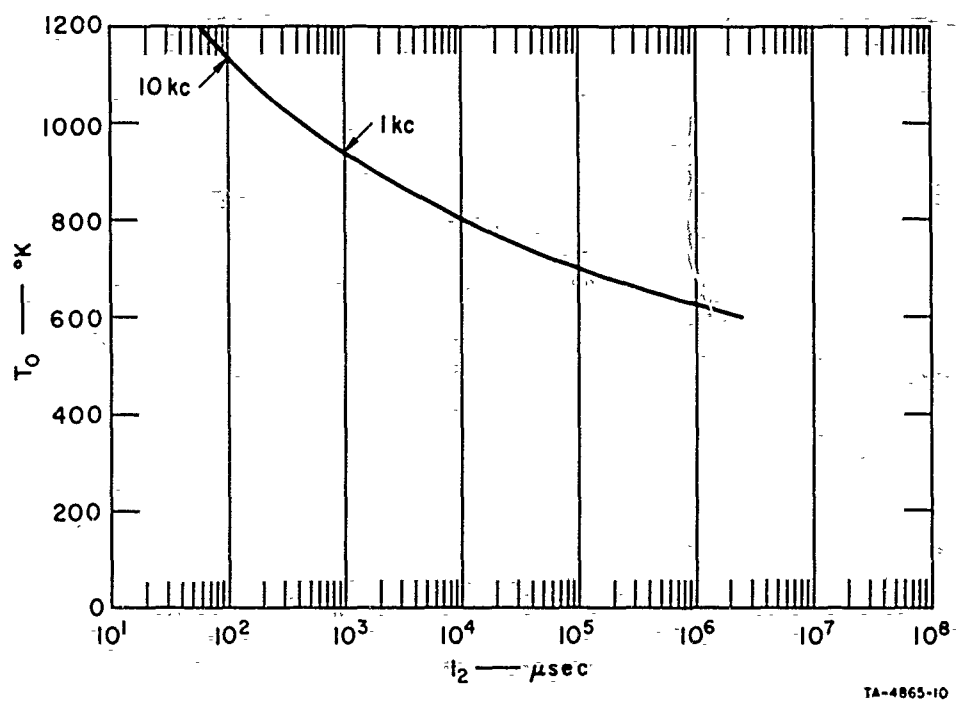


FIG. 14 PLOT OF TIME TO EXPLOSION vs. SURFACE TEMPERATURE FOR AN ALUMINIZED COMPOSITE PROPELLANT

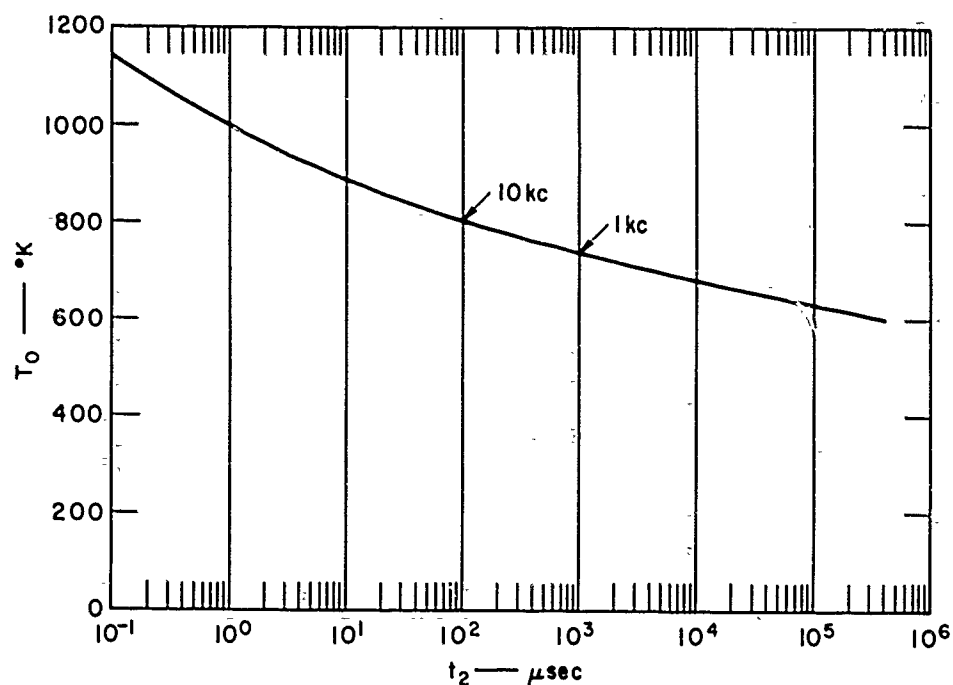


FIG. 15 PLOT OF TIME TO EXPLOSION vs. SURFACE TEMPERATURE FOR AMMONIUM PERCHLORATE

related to the fundamental (or overtones of the) natural acoustic modes in the combustor which may be narrowly tuned by the resonant combustion process.

In view of the fact that we are not able to unequivocally eliminate the thermal explosion response mechanism, it deserves further experimental study since it appears it may explain the intermittent nature of classical secondary peaks.

Granular Diffusion Flame Model

Morrell and Priem²¹ developed, for liquid propellant rocket engines, a practical model based on characteristic times of both mixing processes and chemical reactions which has successfully explained the stability regimes observed when liquid bipropellants are burned. Following discussions with Morrell, it was decided that our own data for heterogeneous composite propellants should be examined using a similar combustion model since the granular diffusion flame model which Summerfield²² proposes for composite propellants phenomenologically resembles the heterogeneous injector element used in liquid propellant rocket engines.

The combustion model we propose as the most acceptable for examining our data in relation to characteristic times of critical processes comprises a solid surface which consists of a regular distribution of discrete sources of deflagrating oxidizer and ablating fuel. These produce respectively a hot oxidizing gas mixture and hot combustible fuel fragments which burn together in a granular diffusion flame. Summerfield has shown that this diffusion flame concept can explain the observed pressure dependence for the burning process of composite propellants; this diffusion flame can also be expected to be velocity-coupled in respect to flow fields and the acoustic or finite amplitude waves present in the combustor. Flow coupling may be identified as the well-known process of erosive burning, with the wave coupling mechanism being responsible for the observed instability phenomenon.

It should be noted that a special problem exists with solid propellants since the propellant feed mechanism is invariably closely coupled with the combustion processes; this is due to the dependence of burning rate on combustor pressure (in the liquid engine it is possible to decouple the propellant feed processes to the combustor). With this point in mind we proceed to examine the characteristic mixing time associated with the granular diffusion flame of the propellant and the wave time in the combustor. Following the method of Povinelli,²³ we may consider the propellant surface as a series of discrete sources with a spacing between element, s , given by the following expression:

$$s = f(d, \theta, Og) \quad (1)$$

where d is the oxidizer mean particle diameter and θ , the oxidizer volume fraction; Og is a particle shape factor. (In our simple comparative analysis we will assume no significant contribution from Og .) Using the simplified model of turbulent burning proposed by Bittker,²⁴ which has been experimentally verified in a liquid engine by Hersch,²⁵ a mixing parameter, α , can be defined as a function of s and the mixing length:

$$\alpha = \mathcal{I}(x/s) \quad (\mathcal{I} \text{ is the intensity of turbulence}) \quad (2)$$

Using mass flow continuity at the surface we obtain, for threshold conditions, a relationship:

$$x = \frac{r_T \rho_s t^*}{\rho^*} \quad (3)$$

where r_T is the linear burning rate of the propellant, ρ_s is the propellant density, t^* is the characteristic combustion time for mixing, and ρ^* is the average gas density of the reactants in the diffusion flame within the combustion zone.

Combining relationships (1), (2), and (3), and relating ρ^* to pressure, we obtain:

$$\alpha = \frac{\mathcal{J} r_T \rho_s R T^* t^*}{M^* P_{T_s}} \quad (4)$$

where T^* is an average temperature characteristic of the combustion zone reactants and M^* is the associated average molecular weight.

Some comment on the values of the parameters assigned the combustion zone reactants is in order. We postulated a mixing length x for the granular diffusion flame; this implies that over this average distance the oxidizing cores of the granular flames taper down to zero. Since the cores contain unburnt gas it appears reasonable to characterize the gas by its entry state from the solid phase. We believe that this entry state can be best characterized by the average surface temperature of the propellant or by temperatures assigned individually to the fuel or oxidant sources in the surface. The oxidizer decomposes to yield reactive intermediates which produce significant amounts of hot decomposition products, whereas the lower volume fraction fuel binder generates a reduced volume of relatively high molecular weight decomposition fragments. (The entry temperature of the fuel fragments may be assumed to be close to that of the oxidizing gases.) Since AP comprises the bulk of the propellant surface, we selected data reported for its surface temperature as the controlling factor.

In this discussion we are in essence de-emphasizing the reactions in the decomposition flame; these may affect the over-all magnitude of parameters used to describe the diffusion flame such as t^* , T^* , and M^* . It is considered, however, that the outstanding success of the Summerfield model of the composite propellant flame implies that these factors may not be limiting; moreover, if reactions occur, the average temperature may closely follow the entry temperature of gases (principally NH_3 and $HClO_4$).

We propose therefore in our argument to assign to T^* the values which would be predicted assuming equilibrium dissociation of ammonium perchlorate at the solid-gas interface of the burning propellant. Powling and Smith²⁰ have shown, by direct experiment, that at pressures up to at least 60 psia, this process is significant. The extrapolated values to rocket operating pressure (Fig. 16) are not inconsistent with estimates by others, e.g., Friedman, et al.,²⁶ or by experimental thermocouple measurement, e.g., Summerfield and Wenograd.²⁷

With the above considerations in mind, Eq. (4) may be rearranged to express the characteristic combustion time for the diffusion flame as:

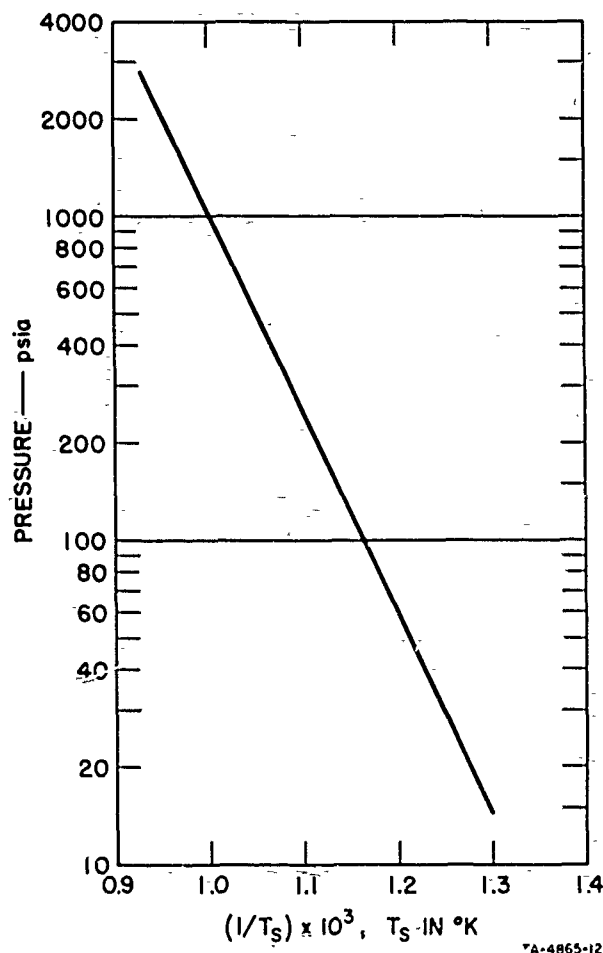


FIG. 16 PREDICTED SURFACE TEMPERATURE — PRESSURE RELATIONSHIP (Powling and Smith data)

$$t^* = \frac{\alpha M^*}{\mathcal{J} \rho_s R} \cdot \frac{s}{r_T T^*} \cdot \frac{P_T}{r_T T^*} \quad (5)$$

For axial instability the wave time in the combustor may be identified as:

$$t_w = \frac{2L}{c} \quad (6)$$

where L is the length of the cavity and c is the velocity of sound. The velocity of sound is best determined experimentally in the burner since many propellants generate multi-phase working fluids and calculation of c from theoretical data is not sufficiently rigid in its derivation.

For assessment of our experimental data we may study the relationship of the characteristic combustion time with the wave time by dividing Eq. (5) by Eq. (6):

$$\frac{t^*}{t_w} = \frac{\alpha M^*}{\mathcal{J} \rho_s R 2L} \cdot \frac{s c}{r_T T^*} \cdot \frac{P_T}{r_T T^*} \quad (7)$$

In the combustor used in our studies the geometry was held constant and the axial wave time was inversely proportional to the velocity of sound.

It is pertinent to examine Eq. (7) on the basis that the boundary between stability and instability is fixed by the requirement for the ratio $\frac{t^*}{t_w}$ to be constant. We find that several categories of variables are present; these are:

- 1) Prime ballistic variables, i.e., P_T and r_T
- 2) Dependent ballistic variables, i.e., T^*
- 3) Principal compositional variables, i.e., d , θ , O_g , ρ_s
- 4) The dependent compositional parameters, M^* and c .

It is tacitly assumed that α and \mathcal{J} are invariant in the granular diffusion model of the burning surface of the composite propellant. (Note, however, that for initiation of instability the generation of the critical axial velocity perturbation required will depend on the pulse characteristics and the chamber pressure.)

Stability Bound Analysis

Examining our data, we found a correlation between the threshold pressure and propellant burning rate, Fig. 6; use of the assigned temperature T^* , as will be seen later, enables an improved correlation to be developed (Fig. 17). Reference to our experimental data on the oxidizer (Appendix A) shows that most propellants have a large weight fraction of particles with the same over-all particle size distribution; however, those propellants containing a large proportion of extremely fine oxidizer burned much faster and were always stable, whereas other propellants

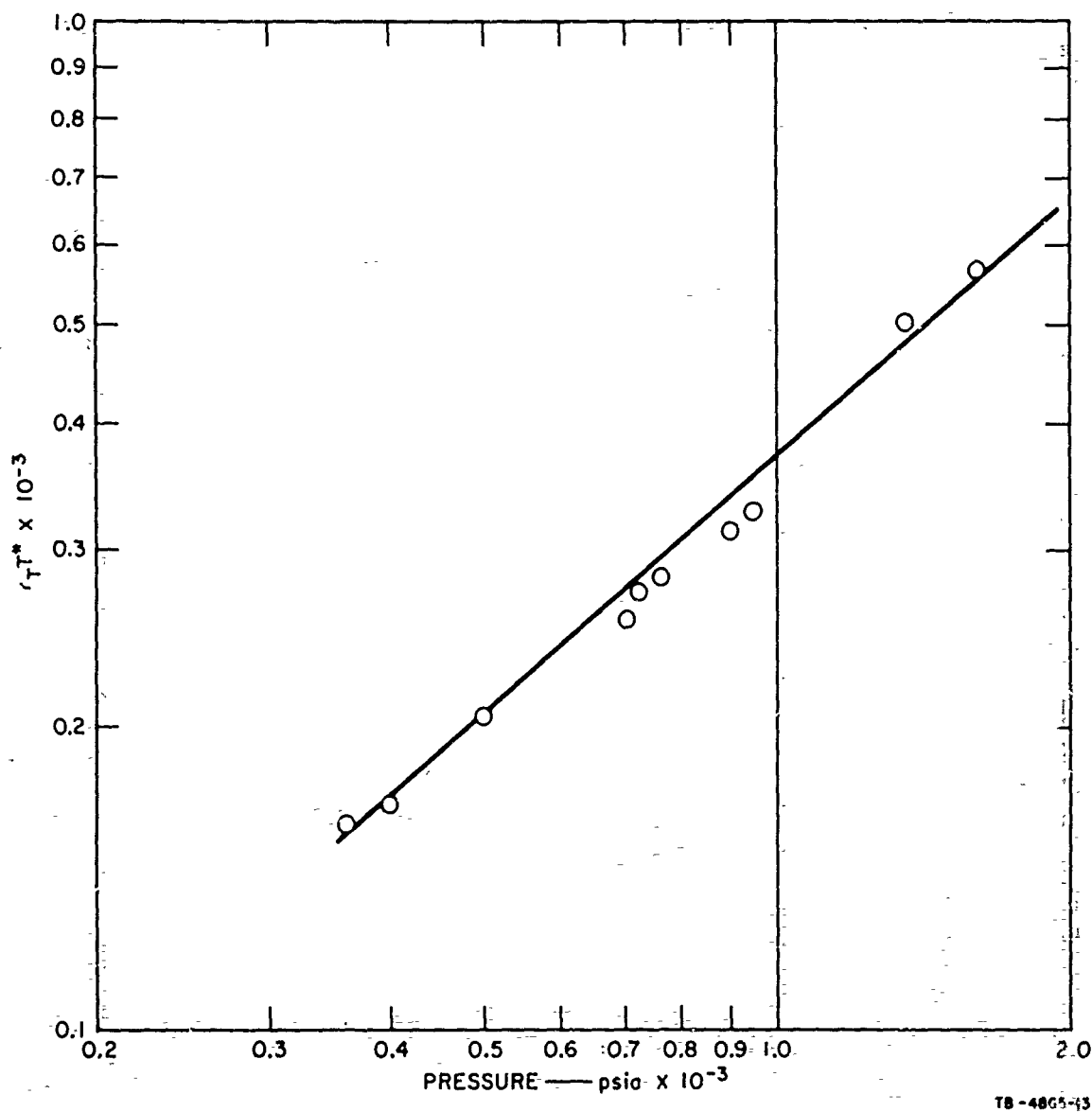


FIG. 17 CORRELATION OF THRESHOLD PRESSURE WITH $r_T T^*$

containing a larger weight fraction of coarse material followed the general trends. It is considered that the small number of large particles did not significantly affect the diffusion flame characteristics which were controlled by the standard bimodal mix. In Appendix A the relationship of our source spacing to propellant oxidizer characteristics is given; for our evaluation here it appears that the values of s , i.e. $f(d, \theta, Og)$, were constant for most propellants. The density of the propellant ρ_s , varies but slightly; similarly, c varies but slightly. The parameter M^* could vary significantly, but for our family of ammonium perchlorate-based propellants, as stated previously, it is considered invariant.

With the foregoing argument in mind the experimentally determined propellant ballistic characteristics at the threshold of instability may be examined in relation to various parameter groupings, namely

- 1) Prime ballistic variables corrected for the dependent ballistic variable T^* (i.e., in comparison of \dot{P}_T with $T^* r_T$)
- 2) Correction for the changes in c , ρ_s , and T^* .

The data cross plot allowing for surface temperature is shown in Fig. 17, and the correlation including c , ρ_s , and T^* is shown in Fig. 18. Tabulated numerical data for the propellants are presented in Table VI.

From an examination of the data it can be concluded that a good data correlation is obtained between propellant burning rate and the instability threshold pressure through the model devised from the Summerfield granular diffusion flame and the ideas derived from the liquid engine injector mixing criteria of Morrell and Priem.

The relationship developed appears to be well verified by the experimental data presented. Of great interest also is the fact that if we assume that resonance occurs over a finite band, then we may predict that the critical combustion time will be increased, leading to instability at the appropriate bound by several factors:

- 1) Increase in pressure at constant burning rate
- 2) Decrease in burning rate at constant pressure
- 3) Increase in the velocity of sound in the combustion products

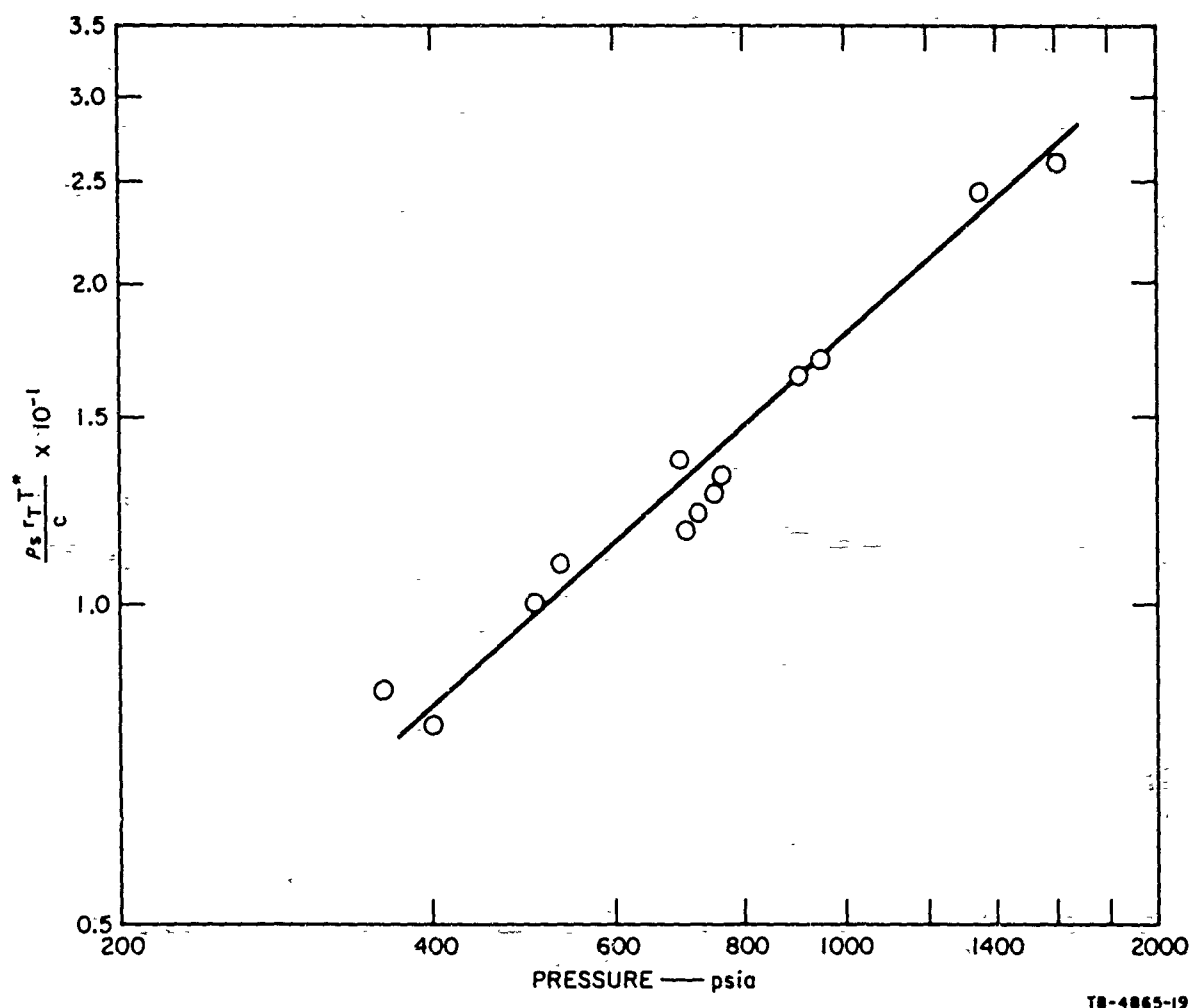


FIG. 18 CORRELATION OF THRESHOLD PRESSURE WITH $\rho_s T^*, r_T$ AND c

- 4) Decrease in propellant density
- 5) Increase in source spacing.

The facts supporting the above comments are:

- 1) All propellants tested which were unstable transitioned to instability as the pressure increased.
- 2) Increase in burning rate invariably produced a more stable propellant (use of catalysts, aluminum addition, or particle size control).
- 3) It has been reported but not yet adequately confirmed in this study that decrease in energy has stabilized the combustion of some propellants.

Table VI

COMPARISON OF THRESHOLD PRESSURE WITH BALLISTIC PARAMETERS

Formulation No.	Threshold Pressure, psi	r_T , ins/sec	T^* , °K	$r_T^* \times 10^{-3}$	ρ_s g/cc	$\rho_s r_T^* \times 10^{-3}$	f, cps	c, fps	$\rho_s r_T^* \times 10^{-1}$
102	950	.325	994	.323	1.72	.556	530	3533	1.57
103	700	.30	975	.292	1.61	.470	500	3333	1.41
104	360	.17	931	.158	1.61	.254	463	3087	.823
105	900	.315	990	.312	1.72	.537	490	3270	1.64
106	1600	.56	1030	.577	1.72	.992	571	3807	2.60
161	750	.275	978	.269	1.72	.463	545	3633	1.27
162	760	.29	980	.284	1.72	.489	555	3699	1.32
166	500	.215	950	.205	1.67	.342	511	3406	1.00
170	1350	.50	1020	.510	1.72	.877	538	3587	2.44
172	530	.24	956	.229	1.64	.377	517	3446	1.09
184	700	.260	975	.253	1.72	.435	557	3713	1.17
186	720	.28	977	.273	1.61	.440	542	3613	1.22
108 PU	400	.18	940	.169	1.59	.269	523	3487	.770

- 4) The higher density aluminized propellants are proportionately more stable.
- 5) A decrease in source spacing (fine oxidizer) produces relatively faster burning and also more stably burning propellants.

Discussion of Compositional Factors

It is considered significant that all the propellants we triggered into instability contained ammonium perchlorate. At the low pressure end of the stability bound, only non-aluminized propellants were found; at the high pressure end aluminized propellants and catalyzed propellants apparently obeyed the same stability criteria. We surmise that at the levels studied, the inclusion of aluminum did not affect the basic mechanism responsible for instability since the combustion time associated with the aluminum was well outside the critical range.

The stability of the potassium and lithium perchlorate propellants can be explained as being due to either their fast burning rate which leads to a very short combustion time or perhaps to the different decomposition mechanism of the oxidizer. We cannot unequivocally select one reason over the other. The stability of fast burning catalyzed ammonium perchlorate propellants is readily explained by the model.

The slow burning ammonium nitrate propellant was found to be stable. Here again stability may be due to its burning rate curve lying beyond the outer bound of a stability band (characteristic of a critical reaction time which is too long). Alternatively, it may be related to a different decomposition mechanism; it is pertinent to note both potassium perchlorate and ammonium perchlorate are reported to melt during burning.

The preliminary and limited data on the nitrasol propellant containing ammonium perchlorate suggest that the instability criteria for a high energy binder will be very different from that for a classical "Summerfield" composite propellant.

Acoustical Instability Theory

The theoretical treatments developed by Hart and McClure¹⁴ have stimulated much experimental work on the measurement of critical parameters

such as the acoustic admittance of the burning propellant surface. Recently the theory has been developed to explain the origin of axial instability in relation to erosive coupling effects of acoustic waves in the cavity of the burning grain. Satisfactory explanations for the presence of the characteristic traveling finite amplitude waves are now available (see for example the work of Hart et al.⁶).

In order to aid in correlating our studies with other work we had the acoustic admittance of two of our more stable fast burning propellants determined. This work, supported by Stanford Research Institute, was carried out by Ryan and Oberg using the University of Utah T-burner. Their detailed results are reported in Appendix B; it appears that the very fast burning potassium perchlorate propellant (PBAN 109) has a lower acoustical admittance than the fast burning ammonium perchlorate propellant (PBAN 111). The burning characteristics of this latter propellant closely resemble the Utah F propellant which has been extensively investigated in the T-burner.

The Utah F propellant is reported as being extremely unstable to pressure-coupled oscillations in the T-burner; our work showed that, in our relatively low loss motor, the equivalent propellant--PBAN 111--was quite stable to 500 cps axial oscillations. While our other similar fast burning propellants have been shown to be readily unstable in the transverse high frequency modes, in the few firings made, we have as yet no instances of PBAN 111 being unstable in the transverse mode.

While the modes of driving for the acoustical oscillations observed during unstable burning have not yet been unequivocally identified, the fact that our stable propellants are shown to possess low acoustical admittances implies that there is no apparent conflict between the acoustical theory proposed and our experimental results.

Application of Experimental Results to Design and Scaling of Rocket Motors

Our experimental study has been concerned primarily with the high energy ammonium perchlorate-based propellants containing up to 15 per cent by weight of aluminum. Previous work has shown, for this type of propellant

in which the rate-controlling reactions are apparently those related to oxidizer decomposition and the diffusion flame between oxidizer and binder, that combustion stability is improved by scale-up of motor size. This generalization does not appear to hold for highly aluminized fuel-rich propellants where the rate-controlling reactions cannot be readily identified. Another problem is that with slow burning aluminum-rich propellants, wave triggered shedding* of molten aluminum can contribute to unstable behavior.

With the above reservations in mind, reference to Fig. 6, which shows the stability bound for the ammonium perchlorate propellants, suggests that in the normal regimes of operation of present day propellants axial instability,** if observed in a motor, may be eliminated by one of two approaches. First of all, a reduction in operating pressure will, for a specific propellant, move it into the stable burning region. Secondly, if operating pressure must be held constant, then a faster burning propellant should be chosen. It is interesting to note that the diffusion flame physical model proposed also predicts the same stability trends. Both these choices may require that the grain geometry be changed if a given thrust time program is to be held to.

Another method of eliminating instability appears to be by reducing the length to diameter ratio of the grain; so far the critical parameters have not been elucidated. Mention was made in a previous section of transverse instability. In our scale motor work, aluminized composite propellants have invariably failed to sustain the transverse, or high frequency, mode of instability. The very high energy aluminized double base propellant could sustain both low frequency axial mode instability and a high frequency transverse mode of instability. It is considered a possibility at this time that this latter phenomenon of transverse instability in an aluminized propellant is associated with the high energy binder; therefore similar stability problems might also be expected with nitro plasticized composite propellants.

* This mechanism was first suggested by E. W. Price; NOTS.

** Also known as Intermediate Frequency Instability (IFI)

Some observations are relevant to the use of potassium perchlorate and ammonium nitrate propellants. Our work confirms that these propellants appear to be stable under the conditions where ammonium perchlorate propellants may burn in an unstable manner. This may be due to the fact that their natural frequencies are outside the band encompassed by the acoustic frequencies of state-of-the-art rocket motors. It may also be due to different combustion reactions at the solid surface of the propellant. If the former, there may be an upper pressure stability bound for certain propellants. Our work indicates that for most of our unstable ammonium perchlorate propellants, this bound, if it exists, is above 3000 psia. As motor free volume increased, there was some indication that oscillation amplitude decreased for certain propellants (see Figs. 5a and b).

In conclusion, it can be stated that, if axial combustion instability (IFI) is observed, then both the experimental data and the theoretical mixing model proposed suggest that it can be eliminated by simple ballistic design changes such as propellant burning rate characteristics, motor operating pressure decrease, or a reduction in grain length to diameter ratio.

VI CONCLUDING REMARKS

The study program covered in this report was deliberately aimed to cover a wide range of propellant compositions typical of those used in aerospace rocket motors. Many facets of the instability problem were uncovered; some of these were examined in great detail because of the ease of formulating propellants with the necessary ballistic properties. The more intractable aspects have to be the subject of further study.

The major conclusion reached has been that a stability bound exists for propellants burned in a scale rocket motor (5 inches I.D. by 40 inches long). This bound is uniquely determined by the relationship between the pressure at which a given propellant can be driven unstable and the associated propellant linear burning rate. A diffusion flame model has been shown to be one possible explanation of the pressure/burning rate stability-dependence observed; other models may also explain the experimental facts and specific experiments are planned in order to discriminate between the possibilities.

The fact that instability is burning rate-dependent is also in accord with independent observations made by Povinelli²⁸ in a small vortex burner.

Future work will seek to clarify further the interaction of homogeneous gas phase reactions, diffusion flame processes, and solid phase reactions in relation to the driving of combustion instability in the different types of solid propellants.

ACKNOWLEDGMENTS

The assistance of George M. Muller and G. Neil Spokes on many specialized aspects of our experimental study is gratefully acknowledged. The numerous discussions held with associated workers in the field of combustion instability have also contributed materially to the success of our studies.

REFERENCES

1. Wimpres, R.N., Internal Ballistics of Solid Fuel Rockets, McGraw-Hill Book Company, 1950, p. 122.
2. Angelus, T.A., Unstable Burning Phenomenon in Double Base Propellants, Progress in Astronautics and Rocketry, Vol. I, Academic Press, 1960, pp. 527-560.
3. Green, L., Jr., Some Properties of a Simplified Model of Solid Propellant Burning, Jet Propulsion 28, 386-392 (1958).
4. Shinnar, R., and Dishonn, M., Heat Transfer Stability Analysis of Solid Propellant Rocket Motors, Progress in Astronautics and Rocketry, Vol. I, Academic Press, 1960, pp. 359-374.
5. Smith, A.G., A Theory of Oscillatory Burning of Solid Propellants Assuming a Constant Surface Temperature, Progress in Astronautics and Rocketry, Vol. I, Academic Press, 1960, pp. 375-392.
6. Hart, R.W., Bird, J.F., Cantrell, R.H., and McClure, F.T., Nonlinear Effects in Instability of Solid Propellant Rocket Motors, AIAA Journal, 2, 1270-1273 (1964).
7. Dickinson, L.A., and Jackson, F., Studies on Combustion of Polyurethane Propellant in Rocket Motors, CONFIDENTIAL, 9th Tripartite AXP Research Conference, Vol. IV, April 1959.
8. Dickinson, L.A., Command Initiation of Finite Wave Axial Combustion Instability in Solid Propellant Rocket Motors, ARS Journal, 32, 643 (1962).
9. Pickford, R.S., and Peoples, R.G., Inherent Stability of the Combustion Process, ARS Preprint 1490-60; ARS 15th AGARD Meeting, Washington, D.C., December 5-8, 1960.
10. Dickinson, L.A., and Jackson, F., Combustion in Solid Propellant Rocket Engines, 5th AGARD Colloquium on Combustion and Propulsion, The Macmillan Company, New York, 1963, pp. 531-550.
11. Dickinson, L.A., Brownlee, W.G., and Jackson, F., CARDE Investigations of Finite Wave Axial Combustion Instability, CARDE Technical Note 1959-62 (U).
12. Swithenbank, J., and Sotter, G., Vortex Generation in Solid Propellant Rockets, AIAA Journal, 2, 1297-1302 (1964).

REFERENCES (Cont'd)

13. Crocco, L., and Cheng, S.I., Theories of Combustion Instability in Liquid Propellant Rocket Motors, AGARD Monograph, No. 8, Butterworth's (London), 1956.
14. Hart, R.W. and McClure, F.T., Combustion Instability: Acoustic Interaction with a Burning Propellant Surface, J. Chem. Phys., 30, 1501-1514 (1959).
15. Sirigano, W.A., and Crocco, L., A Shock Wave Model of Unstable Rocket Combustors, AIAA Journal, 2, 1285-1298 (1964).
16. Frank-Kamenetsky, D.A., Journ. Physic. Chem. Soc. Russia 18, 738 (1939).
17. Clemmow, D.M., and Huffington, J.D., An Extension of the Theories of Thermal Explosion and Its Application to the Oscillatory Burning of Explosives, Rocket Propulsion Department, Technical Note RPD 128, September 1955, Ministry of Supply, London.
18. Gray, P., and Harper, M.J., Thermal Explosions, Trans. Faraday Soc., 55, 581-590 (1959).
19. Gross, D., and Amster, A.B., Thermal Explosions: Adiabatic Self-Heating of Explosives and Propellants, 8th Symposium (International) on Combustion, Williams and Wilkens Company, Baltimore, 1962, pp. 728-734.
20. Powling, J., and Smith, W.A.W., The Surface Temperature of Ammonium Perchlorate Burning at Elevated Pressures, Explosives Research and Development Establishment, Report No. 2-R-63, Ministry of Aviation, London.
21. Morrell, G. and Priem, R.J., Recent Aspects of Rocket Combustion Research; the Proceedings of the NASA University Conference on the Science and Technology of Space Exploration, Vol. II, NASA Sp-11, December 1962, National Aeronautics and Space Administration (Washington, D.C.), pp. 37-42.
22. Summerfield, M., Sutherland, G.S., Webb, M.J., Taback, H.J., and Paul, K.P., Burning Mechanism of Ammonium Perchlorate Propellants, Progress in Astronautics and Rocketry, Vol. I, Academic Press, pp. 141-182.
23. Povinelli, L.A., Effect of Oxidizer Particle Size on Additive Agglomeration, Lewis Research Center, NASA Technical Note D-1438, November 1962.

REFERENCES (Concl'd)

24. Bittker, D.A., An Analytical Study of Turbulent and Molecular Mixing in Rocket Combustion, NACA TN 4321-1958.
25. Hersch, M., Experimental Method of Measuring Intensity of Turbulence in a Rocket Chamber, ARS Journal, 31, 39-45 (1961).
26. Friedman, R., Levy, J.B., and Rumbel, K., AFOSR Technical Note 59173, February 1959.
27. Summerfield, M., Sabadell, A.J., and Wenograd, J., The Measurement of the Temperature Profiles of Burning Solid Propellants by Micro-thermocouples, Technical Report, Contract Nonr 1858 (32), Princeton University, September 1963.
28. Povinelli, L.A., and Heidman, M.F., Study of Transverse Mode Solid Propellant Combustion Instability, Lewis Research Center Technical Progress Report, 20 November 1964.

Appendix A

OXIDIZER PARTICLE SIZE AND SOURCE SPACING CONSIDERATIONS

A realistic physical model for a composite propellant must take into account that it is a polydisperse mixture of oxidizer particles bonded together with a continuous external phase of polymer. Under these conditions it is difficult to decide what parameters should be used to characterize the burning surface of a solid propellant. Since we are attempting to correlate ballistic behavior in terms of Summerfield's granular diffusion flame model, a particle or other surface parameter should, if possible, be selected for each propellant.

Many similar material and surface characterization problems have been encountered in widely differing substances such as rubber fillers, concrete ballast, and coal dust. The parameters suggested have included number mean diameter, volume or weight mean diameter, and surface area mean diameter or specific surface.* The number mean diameter is reported to over-exaggerate the importance of small particles. Propellant formulators have usually chosen weight mean diameter, arbitrarily referred to as the equivalent spherical particle, since this is normally measured by the various test procedures the formulators use. It is interesting to note that certain workers, e.g., developers of British plastic propellant, have consistently favored a different procedure centered on measurement of the specific surface; the good correlation reported between propellant burning rate and specific surface is presumably due to the simple relationship between the average cross-sectional area of a particle and specific surface of the powder.

In view of these past observations, it is our opinion that use of mean particle surface area diameter, designated in the above reference as D_s , and the associated distribution curve of particle surface area is

* Chamot, E. M., Handbook of Chemical Microscopy, J. Wiley & Sons, Inc., 1944, pp. 417-419.

the best way of characterizing oxidizer blends and the ballistics of the derived propellants.

In developing our mixing model (Section V) we used a parameter, s , which is the source spacing within the diffusion flame. For a propellant containing no binder, the distribution curve and its mean value based on particle surface might be used to fix the source spacing if the propellant burned in a heterogeneous manner particle by particle. Real propellants usually contain an organic fuel binder or a mixture of metal fuel and an organic binder. This fuel may be looked upon either as filling the interstices between a system of relatively monodispersed oxidizer particles or as a surface film covering a polydispersed system of particles. Accordingly, if the filler is considered as a system of particles resembling distorted spheres with a thin layer of polymer, we can demonstrate that the polymer film (for normal particle sizes) does not materially affect the source spacing.

Consider now a system of particles in a propellant where the oxidizer weight fraction is θ . Let the oxidizer density be ρ_o and binder density ρ_b . Now in a unit element of propellant

$$\frac{\text{Vol. of oxidizer}}{\text{Vol. of propellant}} = \frac{\theta}{\rho_o} \times \frac{1}{\theta/\rho_o + \frac{1-\theta}{\rho_b}} = \frac{1}{1 + \frac{1-\theta}{\theta} \cdot \frac{\rho_o}{\rho_b}}$$

If the radius of the oxidizer particle is $d/2$ and the corresponding radius of the propellant element is R , then

$$\frac{d/2}{R} = \sqrt[3]{\frac{1}{1 + \frac{1-\theta}{\theta} \cdot \frac{\rho_o}{\rho_b}}}$$

Substituting typical values, for $\theta = 0.87, 0.80$, and 0.75 , for $\rho_o = 1.9$, and for $\rho_b = 1.0$, we find that $\frac{d/2}{R}$ changes from 0.92 to 0.87 to 0.85 . The oxidizer weight fraction, θ , of most of the useful propellants ranges from 0.80 to 0.85 , so the change in center to center spacing of the particles due to binder level variation is less than 5% . This center to center spacing may be taken to be equal to the average source spacing, i.e., $s = 2R$.

The prior discussion has centered principally on the monodisperse equivalent of a typical oxidizer particle size distribution, and it is pertinent to examine the oxidizer blends used in our study in greater detail to see if any of the distributions we were able to study materially affected the source spacing.

The oxidizer grinds used to blend our multi-modal distributions of ammonium and potassium perchlorates are detailed in Figs. A-1 and A-2. The typical bimodal blend used, for example, in propellant PBAN 106 is shown in Fig. A-3, while the representative trimodal blend used in PBAN 184 is shown in Fig. A-4. It will be observed that the median surface area particle size in one case is 103 microns and in the other, 123 microns. A further examination of Figs. A-3 and A-4 reveals that the major fraction of each propellant is encompassed by two particle size bands of 40 to 50 and 100 to 300 microns. It is not unreasonable to suppose that most of the propellants studied had similar responses governed by the predominant source spacing as characterized by the most important particle size bands.

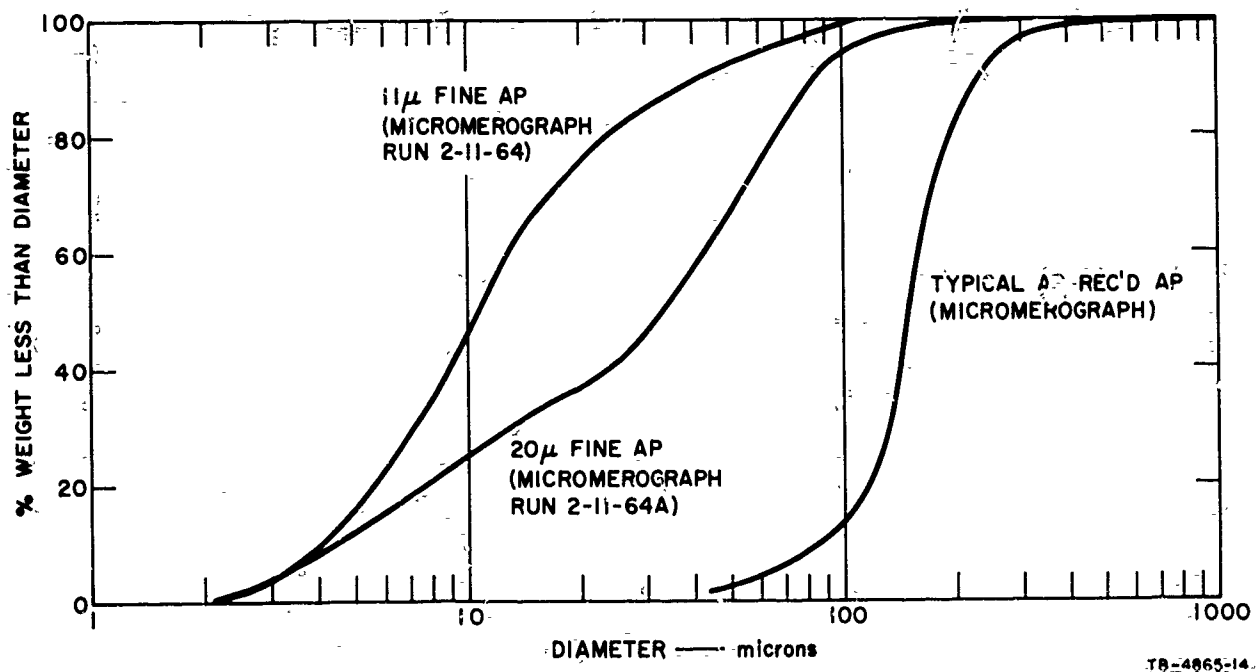


FIG. A-1 PARTICLE SIZE DISTRIBUTION FOR AMMONIUM PERCHLORATE

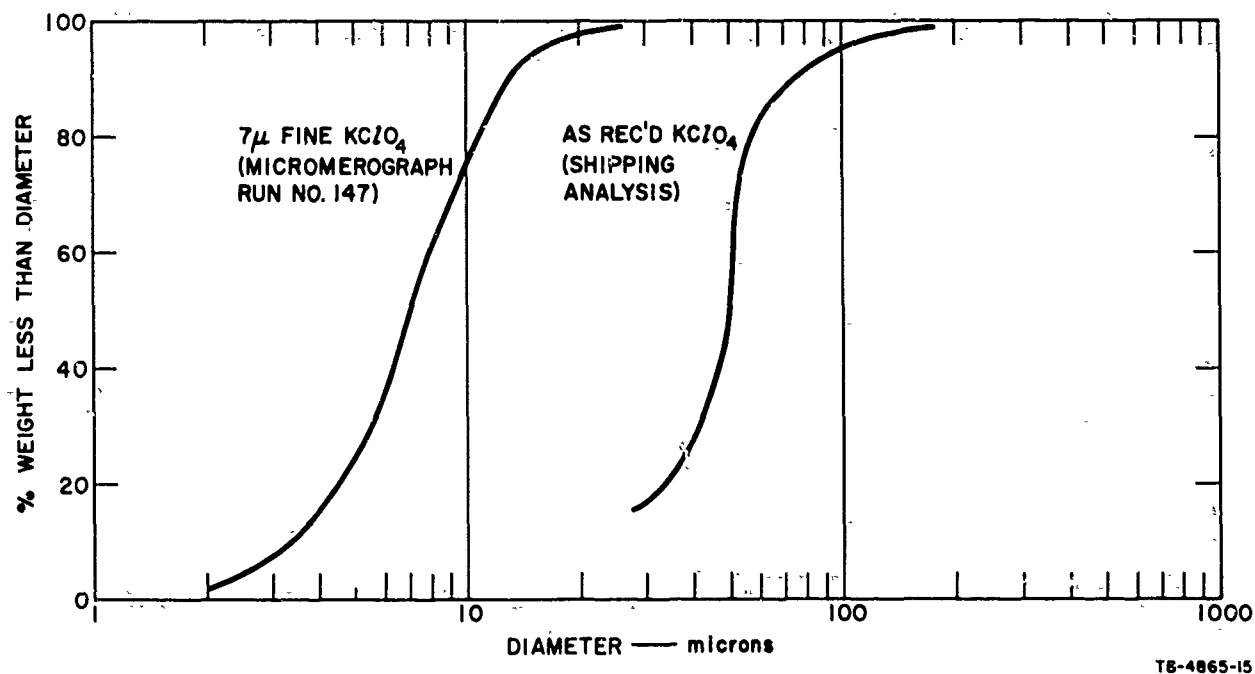


FIG. A-2 PARTICLE SIZE DISTRIBUTION FOR POTASSIUM PERCHLORATE

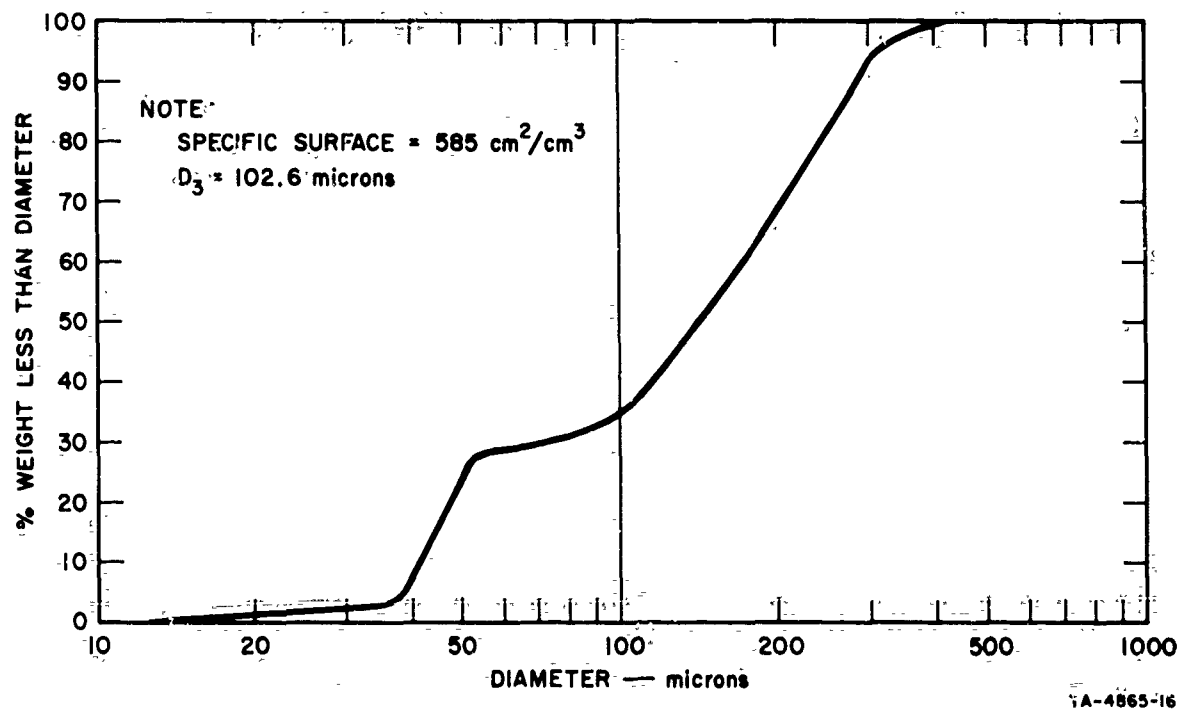


FIG. A-3 PARTICLE SIZE DISTRIBUTION FOR TYPICAL BIMODAL BLEND OF AMMONIUM PERCHLORATE

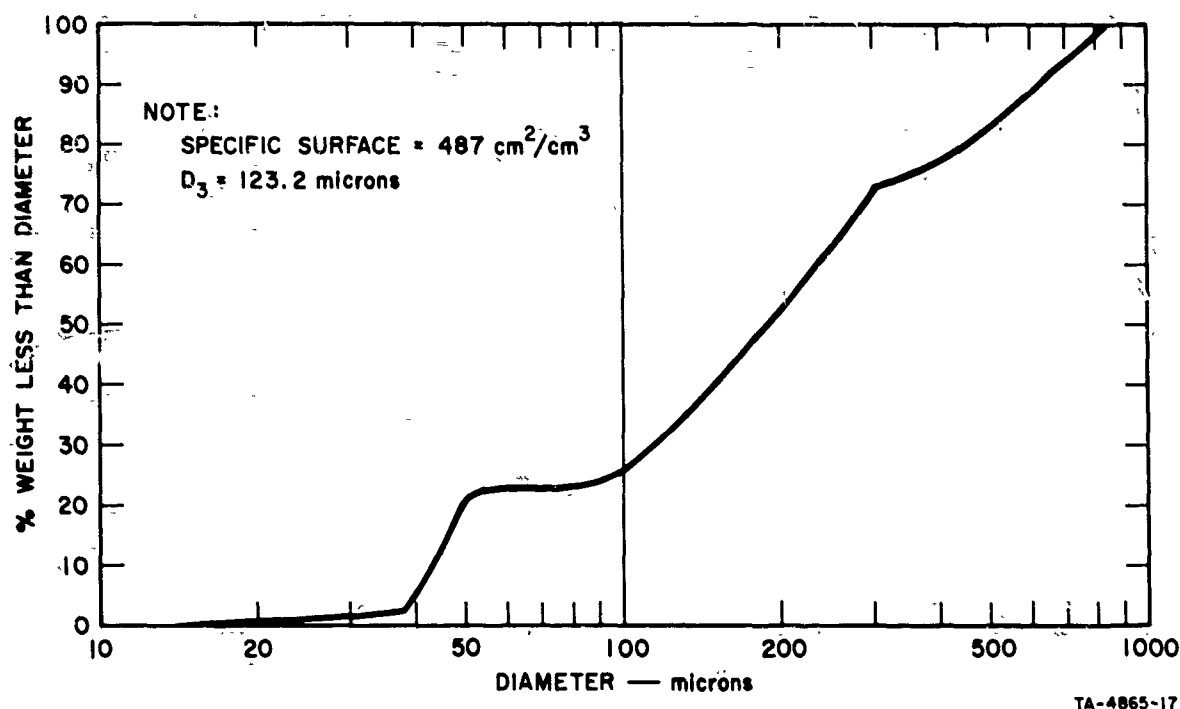


FIG. A-4 PARTICLE SIZE DISTRIBUTION FOR TYPICAL TRIMODAL BLEND OF AMMONIUM PERCHLORATE

An examination of the propellants shows that only one propellant using a mixture of very fine ammonium perchlorate and coarse potassium perchlorate had a median surface area particle size which was appreciably different. The distribution for this propellant, PBAN 189, is shown in Fig. A-5 and here the specific surface median particle size was 9.9 microns. It will be recalled that this was very fast burning and it burned stably in our motor. (An experiment suggested by this discussion would be to add lithium fluoride to this propellant with a view to reducing its burning rate.)

In summary, the seemingly wide formulation changes made, if considered on the basis of surface area median particle size, do not severely test the validity of the model we propose. It can be seen that by virtue of the finite band widths in the particle size distribution that the diffusion flame can possess a broad band response. Consequently, the selectivity

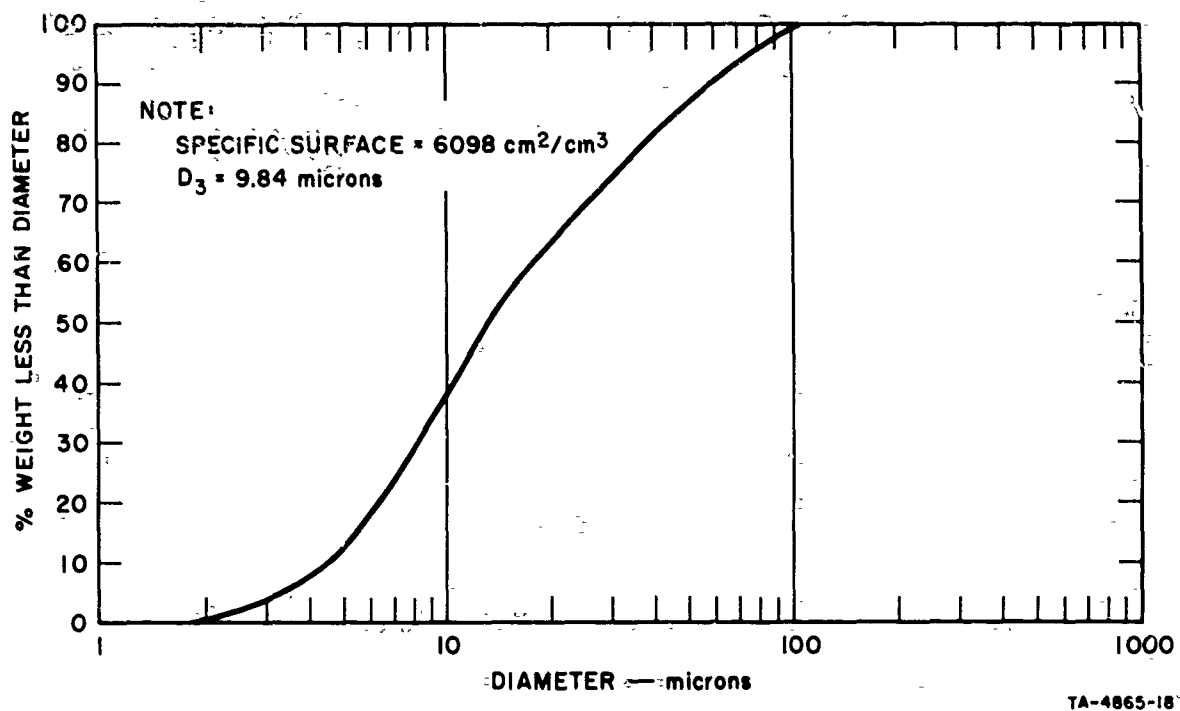


FIG. A-5 PARTICLE SIZE DISTRIBUTION FOR BIMODAL BLEND
 OF AMMONIUM AND POTASSIUM PERCHLORATES

shown in respect of source spacing in Eq. (7) of Section V disappears with a real propellant and the variation in relative distribution may only manifest itself in amplitude effects.

Appendix B

DETERMINATION OF SPECIFIC ACOUSTIC ADMITTANCE FOR SRI PROPELLANTS PBAN 109 AND PBAN 111*

The instability characteristics of SRI propellants PBAN 109 and PBAN 111 have been determined at a pressure of 500 psi and a frequency of 220 ± 20 cps. A side-vented T-burner 1.5 inches in diameter, 40 inches long, with short, end-burning grains was used. It is concluded that in these tests PBAN 111 burned less stably, the response function of the burning surface being about 20 per cent greater than for PBAN 109.

Experimental

A small dump tank was used which pressurized the system to 460 psi before firing. Ignition raised the pressure very quickly to 500 psi, and burning increased the pressure thereafter more slowly.

In all runs it was observed that the ignition transient induced high-amplitude oscillations that obscured the normal oscillation growth; also, the oscillations died away before burning was complete. Two preliminary conclusions, therefore, were that the conventional use of the T-burner data was not possible, and that neither propellant could supply driving energy in excess of burner losses. No assurance of stability can be taken from the second conclusion; Utah F propellant, prohibitively unstable for operational use, will not sustain oscillations under these circumstances either.

It was recognized that decay constants for diminishing oscillations after the ignition pulse can be utilized in the same way as growth constants. Decay constants were measured for the igniter (Utah F propellant sawdust) alone, then for each propellant in runs with one grain and with two grains. Decay constants were measured when oscillations were at low amplitude--after the initial nonlinear decay but before the mean chamber pressure rose significantly.

* Determinations carried out at the University of Utah and reported in a letter from N. W. Ryan, dated January 18, 1965.

Theory

For background information, see the paper by Coates, Hertton, and Ryan, AIAA Journal, 2, 1119 (1964). We use the equation

$$\alpha_n = \alpha_0 + 2nKf$$

where α_n is the growth constant, $d \ln |p| / dt$, for a firing with n grains ($n = 0, 1$, or 2); f is the frequency; and K is the real part of the specific acoustic admittance of the burning surface, defined as positive when combustion amplifies the signal. $\alpha_0, \alpha_1, \alpha_2$ were obtained from pressure-time traces. From

$$\begin{aligned}\alpha_0 &= \alpha_0 \\ \alpha_1 &= \alpha_0 + 2Kf \\ \alpha_2 &= \alpha_0 + 4Kf\end{aligned}$$

we obtain three equations for Kf ,

$$Kf = \frac{\alpha_1 - \alpha_0}{2} = \frac{\alpha_2 - \alpha_0}{4} = \frac{\alpha_2 - \alpha_1}{2}$$

Results and Discussion

Table B-1 summarizes the results, showing maximum deviations of measured α values. Mean deviations would make the results much more impressive, but they are not regarded as significant. The determination of α_0 and α_1 as the slopes of $\ln |p|$ vs. t plots can be made with errors less than the differences from one run to the next.

The two-grain firings were the least satisfactory. It was difficult to measure α with confidence because the decay was slow enough that sometimes the chamber pressure had risen to 600 psi or more by the time the oscillations were in the linear range. In the case of PBAN 111, oscillation amplitude stayed steady at a low level for a short time, finally decaying at high mean pressure. It was judged that α_2 was, therefore, zero at the conditions of interest, rather than -3.6 sec^{-1} estimated for initial (probably nonlinear) decay.

Table B-2 shows Kf values computed as shown above. Because the frequencies were not all the same, there is some question about the

actual values of the acoustic admittance. Nevertheless, it is certainly legitimate to compare the propellants.

Table B-1
SUMMARIZED RESULTS

	Number of Firings	Frequency cps	α sec ⁻¹
Igniter only	3	180	-19.8 \pm 0.4
Propellant 109			
One grain	3	220	-11.8 \pm 3.5
Two grains	3	240	- 3.8 \pm 0.9
Propellant 111			
One grain	4	205	- 8.4 \pm 1.0
Two grains	1	---	0*
Utah F Propellant			
One grain ¹	1	244	-8.4

* Measured value, -3.6 sec⁻¹. See text.

Table B-2
SPECIFIC ACOUSTIC ADMITTANCE

	Kf (sec ⁻¹) for		
	Propellant 109	Propellant 111	Utah F
$\frac{\alpha_1 - \alpha_0}{2}$	4.0	5.7	5.7
$\frac{\alpha_2 - \alpha_0}{4}$	4.0	5.0	---
$\frac{\alpha_2 - \alpha_1}{2}$	4.0	4.2	---

Utah F propellant was used to prove out the apparatus, and it appears to be very similar to PBAN 111. The most reliable figures, first row in Table B-2, indicate that PBAN 111, with a specific acoustic admittance about 40 per cent greater, is significantly less stable than PBAN 109. An average for both columns of figures indicates a 20 per cent higher value for PBAN 111. Probably α_2 is slightly greater than zero for PBAN 111. A positive value cannot be detected by the method used. If $\alpha_2 = 3.0$ sec.⁻¹, then all three Kf values are 5.7 sec.⁻¹.

**STANFORD
RESEARCH
INSTITUTE**

**MENLO PARK
CALIFORNIA**

Regional Offices and Laboratories

Southern California Laboratories

820 Mission Street
South Pasadena, California

Washington Office

808-17th Street, N.W.
Washington 6, D.C.

New York Office

270 Park Avenue, Room 1770
New York 17, New York

Detroit Office

1025 East Maple Road
Birmingham, Michigan

European Office

Pelikanstrasse 37
Zurich 1, Switzerland

Japan Office

c/o Nomura Securities Co., Ltd.
1-1 Nihonbashidori, Chuo-ku
Tokyo, Japan

Representatives

Toronto, Ontario, Canada

Cyril A. Ing
Room 710, 67 Yonge St.
Toronto 1, Ontario, Canada

Milan, Italy

Lorenzo Franceschini
Via Macedonio Melloni, 49
Milano, Italy